INTERNATIONAL JOURNAL OF
NUMERICAL ANALYSIS AND MODELING
Volume 12, Number 3, Pages 476–515

FLOW AND TRANSPORT WHEN SCALES ARE NOT SEPARATED: NUMERICAL ANALYSIS AND SIMULATIONS OF MICRO- AND MACRO-MODELS

MAŁGORZATA PESZYŃSKA, RALPH E. SHOWALTER, AND SON-YOUNG YI

Abstract. In this paper, we consider an upscaled model describing the multiscale flow of a single-phase incompressible fluid and transport of a dissolved chemical by advection and diffusion through a heterogeneous porous medium. Unlike traditional homogenization or volume averaging techniques, we do not assume a good separation of scales. The new model includes as special cases both the classical homogenized model and the double porosity model, but it is characterized by the presence of additional memory terms which describe the effects of local advective transport as well as diffusion. We study the mathematical properties of the memory (convolution) kernels presented in the model and perform rigorous stability analysis of the numerical method to discretize the upscaled model. Some numerical results will be presented to validate the upscaled model and to show the quantitative significance of each memory term in different regimes of flow and transport.

Key words. Upscaled model, double-porosity, memory terms, solute transport, non-separated scale, stability.

1. Introduction

We are concerned with advection-diffusion-dispersion equations when studying the flow of a single-phase incompressible fluid and transport of contaminant through heterogeneous porous media. The heterogeneities are represented by two different porous materials. In particular, we do not assume a good separation of scales. In [15], Peszyńska and Showalter derived a discrete version of the double-porosity model with various memory (convolution) terms for the coupled flow-transport equation without assuming a well-defined separation of scales in the porous medium. This model has been numerically studied in [20], where different tailing effects due to the memory terms were observed and the quantitative significance of each memory term in different regimes of flow and transport was studied. However, no analysis for the numerical methods used for the upscaled model was presented in [20]. The main purpose of this paper is to present a rigorous mathematical analysis of the numerical methods that are used to discretize the upscaled model proposed in [15].

For the numerical discretization of the upscaled model with convolution terms, we used the cell-centered finite difference (CCFD) method combined with the product integration rule for the convolution terms in which both the primary and secondary advection terms are approximated using the upwind method. Moreover, the (primary) advection was treated explicitly while the (primary) diffusion and all of the memory terms are treated implicitly in time. Our stability analysis will be given only for the 1d version of the upscaled model.

Received by the editors July 2, 2014 and, in revised form, November 23, 2014.
2000 *Mathematics Subject Classification.* 35B27, 35R09, 75S05, 74Q15, 65M12, 65M06.
This work was supported by the U.S. Department of Energy, Office of Science, Multiscale Mathematics Initiative under Award 98089. Research by Peszyńska was also partially supported by the National Science Foundation under Grant DMS-0511190 R.E. Showalter was partially supported by the U.S. Department of Energy, Office of Science under Award 98089 and Award 9001997.

Known results on numerical analysis of integro-partial differential equations and more general problems with memory terms include those in [18, 9, 10, 19, 12, 11]. All of these papers deal with memory terms of the form $\beta * Lu$, where L is a self-adjoint spatial differential operator. Moreover, all but [10] assume that the kernels β are bounded and monotone. On the other hand, in [13], Peszyńska considered a weakly singular memory term of the form $\beta * u_t$ in a parabolic equation with a self-adjoint elliptic part. Later, in [14], she also considered a memory term with weakly singular β in a first order hyperbolic equation.

For our analysis, we first investigate the qualitative behavior of the convolution kernels present in our model. We carefully represent the kernels in series representations and study their qualitative properties analytically. Unlike the monotone double-porosity and secondary advection kernels, the secondary diffusion kernel is found to be only piecewise monotone. Our mathematical findings on the properties of the convolution kernels will be confirmed numerically.

Using some assumptions on the convolution kernels based on the above findings, we perform stability analysis of our numerical methods for the upscaled model. First, we perform von-Neumann analysis for the upscaled model defined on an infinite domain $\mathbb{R}$. We study a simple version of the problem with only the double-porosity term first, then include additional memory terms, *i.e.*, the secondary advection and secondary diffusion terms, one by one. It is shown that the upwind-memory scheme we employ for our 1d upscaled model with all memory terms is (ultra-) weakly stable. We also discuss stability using the method of lines (MOL).

The rest of the paper is organized as follows: in Section 2, we describe the model problem for a heterogeneous system with combined fast and slow flow regimes. Then, in Section 3, we present the upscaled model with various memory terms for the coupled flow-transport equation that was developed in [15]. In Section 4, we investigate the qualitative properties of the memory kernels using Fourier series representations. Section 5 is devoted to stability analysis of the numerical discretization of the upscaled model using von-Neumann stability analysis and MOL. Finally, in Section 6, we present some numerical results.

2. The Model Problem

Let Ω be a two-dimensional heterogeneous porous medium containing two disjoint flow regimes. The subscripts f and s are associated with the fast and slow regions Ω_f and Ω_s, respectively. These are disjoint open sets covering Ω, $\overline{\Omega} = \overline{\Omega_f} \cup \overline{\Omega_s}$, with an interface $\Gamma_{fs} = \partial\Omega_f \cap \partial\Omega_s$. The region Ω_f is connected, but $\Omega_s = \cup_{i=1}^{N_{\text{incl}}} \Omega_{is}$ is a union of disjoint connected regions Ω_{is}.

Assume that Ω is covered by a union of rectangular subdomains Ω_i, $i = 1, \ldots, N_{\text{incl}}$, with each Ω_i containing exactly one inclusion Ω_{is}. Let $\Omega_{if} = \Omega_i \cap \Omega_f$ be the fast part surrounding Ω_{is} and let $\Gamma_i = \partial\Omega_{is} \cap \partial\Omega_{if}$ denote the local interfaces so that $\Omega_i = \Omega_{is} \cup \Omega_{if} \cup \Gamma_i$ and $\Gamma_{fs} = \cup_i \Gamma_i$. Let us assume that each Ω_i is congruent to a generic cell Ω_0 which contains the fast flow region Ω_{0f} surrounding the slow flow region Ω_{0s}. We also denote the volume fraction of the fast part by $\theta_f = \frac{|\Omega_{0f}|}{|\Omega_0|}$ and analogously $\theta_s = \frac{|\Omega_{0s}|}{|\Omega_0|} = 1 - \theta_f$.

Now, we describe the microscopic model of the flow and solute transport in the heterogeneous porous medium, with porosity and permeability discontinuous across

the interface Γ_i. The flow is described by conservation of mass and Darcy's law:

$$\nabla \cdot \mathbf{v}_f = 0, \qquad \mathbf{v}_f = -\mathbf{K}_f \nabla p_f, \qquad \mathbf{x} \in \Omega_f, \tag{1a}$$

$$\nabla \cdot \mathbf{v}_i = 0, \qquad \mathbf{v}_i = -\mathbf{K}_s \nabla p_i, \qquad \mathbf{x} \in \Omega_{is},\ i = 1, \ldots, N_{\text{incl}}, \tag{1b}$$

$$p_i = p_f, \qquad \mathbf{v}_i \cdot \mathbf{n} = \mathbf{v}_f \cdot \mathbf{n}, \qquad \mathbf{x} \in \Gamma_i, \tag{1c}$$

where $\mathbf{v}$ and p are the velocity and the pressure of the flow, respectively. The coefficient $\mathbf{K}$ is the permeability of the porous medium. The solute transport equation is an advection-diffusion-dispersion system

$$\phi_f \frac{\partial u_f}{\partial t} - \nabla \cdot (\mathbf{D}_f \nabla u_f - \mathbf{v}_f u_f) = 0,\ \mathbf{x} \in \Omega_f, \tag{2a}$$

$$\phi_i \frac{\partial u_i}{\partial t} - \nabla \cdot (\mathbf{D}_i \nabla u_i - \mathbf{v}_i u_i) = 0,\ \mathbf{x} \in \Omega_{is},\ i = 1, \ldots, N_{\text{incl}}, \tag{2b}$$

$$u_i = u_f, \quad (\mathbf{D}_f \nabla u_f - \mathbf{v}_f u_f) \cdot \mathbf{n} = (\mathbf{D}_i \nabla u_i - \mathbf{v}_i u_i) \cdot \mathbf{n},\ \mathbf{x} \in \Gamma_i. \tag{2c}$$

Here, u is the solute concentration and ϕ is the porosity of the medium. The diffusion-dispersion tensor in each region has the form

$$\mathbf{D} = \mathbf{D}(\mathbf{v}) \equiv \phi \left[d_{\text{m}} \mathbf{I} + |\mathbf{v}| (d_{\text{l}} \mathbf{E}(\mathbf{v}) + d_{\text{t}} (\mathbf{I} - \mathbf{E}(\mathbf{v}))) \right]. \tag{3}$$

Here, d_m, d_l, d_t are coefficients of molecular diffusivity, longitudinal and transversal dispersivity, respectively, and the dispersion tensor $\mathbf{E}(\mathbf{v}) = \frac{1}{|\mathbf{v}|^2} v_i v_j$ is a rank two tensor.

3. The Upscaled Coupled Flow-Advection-Diffusion Model With Memory Terms

We shall describe the discrete version of the double-porosity model with various memory terms for the coupled flow-transport equation as developed in [15]. To describe the upscaled flow equation, we first define the upscaled permeability tensor $\mathbf{K}^*$ as follows:

$$(\mathbf{K}^*)_{jk} = \frac{1}{|\Omega_0|} \int_{\Omega_{0f}} (\mathbf{K}_f)_{jm}(\mathbf{y})(\delta_{mk} + \partial_m \omega_k(\mathbf{y}))\, dA, \tag{4}$$

where the Ω_0-periodic function $\omega_k(\mathbf{y})$ is defined as the solution of the periodic cell problem

$$\begin{cases} -\nabla \cdot \nabla \omega_j(\mathbf{y}) = 0, & \mathbf{y} \in \Omega_{0f} \\ \nabla \omega_j(\mathbf{y}) \cdot \mathbf{n} = -\mathbf{e}_j \cdot \mathbf{n}, & \mathbf{y} \in \Gamma_{fs}. \end{cases} \tag{5}$$

The discrete double-porosity model that we employ here uses a local affine approximation on the interfaces which enables the model to capture the effects of advection and secondary diffusion.

To be precise, we define $\mathbf{\Pi}_1 : H_0^1(\Omega) \to \prod_{i=1}^{N_{\text{incl}}} H^{\frac{1}{2}}(\Gamma_i)$ such that, for $i = 1, \cdots, N_{\text{incl}}$, and $\mathbf{s} \in \Gamma_i$,

$$(\mathbf{\Pi}_1 w)_i(\mathbf{s}) \equiv \frac{1}{|\Omega_i|} \left(\int_{\Omega_i} w(\mathbf{y})\, dA + \sum_{k=1}^{2} \left[\int_{\Omega_i} \partial_k w(\mathbf{y})\, dA \right] (s_k - (\mathbf{x}_i^c)_k) \right),\ \mathbf{s} \in \Gamma_i. \tag{6}$$

Here, $\mathbf{x}_i^c$ is the centroid of Ω_i. Then, we can show that the dual Π_1' to $\mathbf{\Pi}_1$ satisfies the following: for $\mathbf{q}_i$ smooth on Ω_{is}

$$\Pi_1'((\mathbf{q}_i\cdot\mathbf{n})_i)(\mathbf{x}) = \sum_i \hat{\chi}_i(\mathbf{x})\frac{1}{|\Omega_i|}\int_{\Omega_{is}} \nabla\cdot\mathbf{q}_i(\mathbf{x})dA \\ -\nabla\cdot\sum_i \hat{\chi}_i(\mathbf{x})\frac{1}{|\Omega_i|}\int_{\Omega_{is}}(\nabla\cdot\mathbf{q}_i)(\mathbf{y}-\mathbf{x}^c)dA - \nabla\cdot\sum_i \hat{\chi}_i(\mathbf{x})\frac{1}{|\Omega_i|}\int_{\Omega_{is}}\mathbf{q}_i dA, \tag{7}$$

where $\hat{\chi}_i(\mathbf{x})$ denotes the characteristic function of the cell Ω_i.

Finally, the upscaled system for the flow is as follows:

$$\nabla\cdot\overline{\mathbf{v}^*} \equiv -\Pi_1'\left((\mathbf{v}^*{}_i\cdot\mathbf{n}_i)_{i=1}^{N_{\text{incl}}}\right) + \nabla\cdot\mathbf{v}^* = 0, \tag{8a}$$

$$\mathbf{v}^* = -\mathbf{K}^*\nabla p^*, \quad \mathbf{x}\in\Omega, \tag{8b}$$

$$\nabla\cdot\mathbf{v}_i^* = 0,\ i=1,\cdots,N_{\text{incl}} \tag{8c}$$

$$\mathbf{v}_i^* = -\mathbf{K}_s\nabla p_i^*, \quad \mathbf{y}\in\Omega_{is} \tag{8d}$$

$$p^*{}_i|_{\Gamma_i} = (\mathbf{\Pi}_1(p^*))_i\,. \tag{8e}$$

We can rewrite the above system by using $\overline{\mathbf{v}^*}$ and a coefficient $\overline{\mathbf{K}^*} = \mathbf{K}^* + \theta_s\mathbf{K}_s$

$$\nabla\cdot\overline{\mathbf{v}^*} = 0, \quad \mathbf{x}\in\Omega, \tag{9a}$$

$$\overline{\mathbf{v}^*} = -\overline{\mathbf{K}^*}\nabla p^*, \tag{9b}$$

$$\nabla\cdot\mathbf{v}_i^* = 0, \quad \mathbf{y}\in\Omega_{is},\ i=1,\cdots,N_{\text{incl}}, \tag{9c}$$

$$\mathbf{v}_i^* = -\mathbf{K}_s\nabla p_i^*, \quad \mathbf{y}\in\Omega_{is}, \tag{9d}$$

$$p_i^*|_{\Gamma_i} = (\mathbf{\Pi}_1(p^*))_i. \tag{9e}$$

In order to describe the upscaled transport system with memory terms in a convolution form, consider a representative function $r^0 = r^0(\mathbf{y},t)$ with *constant* boundary input which is the solution of the initial-boundary-value problem

$$\begin{cases} \phi_s\frac{\partial r^0}{\partial t} - \nabla\cdot(D\nabla r^0 - \mathbf{v}r^0) &= 0, \quad \mathbf{y}\in\Omega_{0s}, \\ r^0(\mathbf{y},0) &= 0, \quad \mathbf{y}\in\Omega_{0s}, \\ r^0(\mathbf{y},t) &= 1, \quad \mathbf{y}\in\Gamma_0. \end{cases} \tag{10}$$

We defined the first kernel function by

$$\mathcal{T}^{00}(t) \equiv \frac{1}{|\Omega_0|}\int_{\Omega_{0s}} \phi_s\frac{\partial r^0(\mathbf{y},t)}{\partial t}dA \tag{11}$$

Additional representative functions, $r^k = r^k(\mathbf{y},t)$ for $k=1,2$, with *affine* boundary input were defined as the solutions of

$$\begin{cases} \phi_s\frac{\partial r^k}{\partial t} - \nabla\cdot(D\nabla r^k - \mathbf{v}r^k) &= 0, &\mathbf{y}\in\Omega_{0s}, \\ r^k(\mathbf{y},0) &= 0, &\mathbf{y}\in\Omega_{0s}, \\ r^k(\mathbf{y},t) &= (\mathbf{y}-\mathbf{x}_0^c)_k, &\mathbf{y}\in\Gamma_0. \end{cases} \tag{12}$$

Then we constructed kernels arising from various averages of r^k. First, we used the averages of rate of change in time as above to define *averaged content rates*

$$\mathcal{T}^{k0}(t) \equiv \frac{1}{|\Omega_0|}\int_{\Omega_{0s}} \phi_s\frac{\partial r^k}{\partial t}(\mathbf{y},t)\,dA, \quad k=0,1,2, \tag{13}$$

where $\mathcal{T}^{00}$ defined previously in (11) is included for completeness. Next, the kernels $\mathcal{T}^{k1}, \mathcal{T}^{k2}$ for *first moment rates* were defined as

$$\mathcal{T}^{kj}(t) \equiv \frac{1}{|\Omega_0|}\int_{\Omega_{0s}} \phi_s \frac{\partial r^k}{\partial t}(\mathbf{y},t)(\mathbf{y}-(\mathbf{x}_0^C))_j \, dA, \quad j=1,2;\ k=0,1,2. \tag{14}$$

Finally, for each $r^k, k=0,1,2$ we specify *averaged flux*

$$\mathbf{S}^k(t) \equiv (S^{k1}, S^{k2}) \equiv \begin{bmatrix} S^{k1} \\ S^{k2} \end{bmatrix} \equiv \frac{1}{|\Omega_0|}\int_{\Omega_{0s}} (D\nabla r^k(\mathbf{y},t) - \mathbf{v} r^k(\mathbf{y},t))\, dA. \tag{15}$$

In summary, we defined the total of fifteen geometry-based and time-dependent kernels: nine zero'th and first order moments $\mathcal{T}^{k0}, \mathcal{T}^{k1}, \mathcal{T}^{k2}$ of $r^k, k=0,1,2$ and six flux averages S^{k1}, S^{k2} for $k=0,1,2$. We note that many of these kernels may vanish due to symmetry when $\mathbf{v}=\mathbf{0}$. They are used to express the upscaled model

$$\begin{aligned} &\phi^* \frac{\partial u^*}{\partial t} + \mathcal{T}^{00} * \frac{\partial u^*}{\partial t} \\ &\quad + (\mathcal{T}^{10}, \mathcal{T}^{20}) * \nabla \frac{\partial u^*}{\partial t} - \nabla \cdot \left((\mathcal{T}^{01}, \mathcal{T}^{02}) * \frac{\partial u^*}{\partial t} \right) - \nabla \cdot \left((S^{01}, S^{02}) * \frac{\partial u^*}{\partial t} \right) \\ &\qquad - \nabla \cdot \left(\begin{bmatrix} \mathcal{T}^{11} & \mathcal{T}^{12} \\ \mathcal{T}^{21} & \mathcal{T}^{22} \end{bmatrix} * \nabla \frac{\partial u^*}{\partial t} \right) - \nabla \cdot \left(\begin{bmatrix} S^{11} & S^{12} \\ S^{21} & S^{22} \end{bmatrix} * \nabla \frac{\partial u^*}{\partial t} \right) \\ &\qquad\qquad - \nabla \cdot (\mathbf{D}^* \nabla u^* - \mathbf{v}^* u^*) = 0, \end{aligned} \tag{16}$$

or, after we collect similar terms,

$$\phi^* \frac{\partial u^*}{\partial t} + \mathcal{T}^{00} * \frac{\partial u^*}{\partial t} + \Xi * \nabla \frac{\partial u^*}{\partial t} - \nabla \cdot \left(\Psi * \nabla \frac{\partial u^*}{\partial t} \right) - \nabla \cdot (\mathbf{D}^* \nabla u^* - \mathbf{v}^* u^*) = 0, \tag{17}$$

in which the combined kernels are given by

$$\phi^* + \mathcal{T}^{00} - \nabla \cdot \left((\mathcal{T}^{01}, \mathcal{T}^{02}) + (S^{01}, S^{02}) \right), \tag{18a}$$

$$\Xi \equiv (\mathcal{T}^{10}, \mathcal{T}^{20}) - \left((\mathcal{T}^{01}, \mathcal{T}^{02}) + (S^{01}, S^{02}) \right), \tag{18b}$$

$$\Psi \equiv \begin{bmatrix} \mathcal{T}^{11} & \mathcal{T}^{12} \\ \mathcal{T}^{21} & \mathcal{T}^{22} \end{bmatrix} + \begin{bmatrix} S^{11} & S^{12} \\ S^{21} & S^{22} \end{bmatrix}. \tag{18c}$$

The first reduces to $\phi^* + \mathcal{T}^{00}$ since the remaining terms are functions of t only.

4. Series Representations of the Kernels

4.1. The constant representative r^0. It is useful to consider the complementary function $r(\mathbf{y},t) = 1 - r^0(\mathbf{y},t)$ which is the solution of the initial-boundary-value problem

$$\begin{cases} \phi \frac{\partial r}{\partial t} - \nabla \cdot (D\nabla r - \mathbf{v} r) &= 0, \quad \mathbf{y} \in \Omega_{0s}, \\ r(\mathbf{y},0) &= 1, \quad \mathbf{y} \in \Omega_{0s}, \\ r(\mathbf{y},t) &= 0, \quad \mathbf{y} \in \Gamma_0, \end{cases} \tag{19}$$

with homogeneous boundary conditions. We have suppressed the subscripts. Note that all coefficients are constants.

Separation of variables in (19) leads to the *eigenvalue problem*

$$-\nabla \cdot (D\nabla \xi - \mathbf{v}\xi) = \phi \lambda \xi \text{ in } \Omega_{0s},\ \xi = 0 \text{ on } \Gamma_0. \tag{20}$$

In order to eliminate the first-order terms, make a change of variable

$$\begin{aligned} \xi(\mathbf{y}) &= e^{\mu \cdot \mathbf{y}} \tilde{\xi}(\mathbf{y}) \\ \nabla \xi &= e^{\mu \cdot \mathbf{y}} (\nabla \tilde{\xi} + \mu \tilde{\xi}) \end{aligned} \tag{21}$$

to get successively

$$
\begin{aligned}
&-\nabla\cdot(e^{\mu\cdot\mathbf{y}}(D\nabla\tilde{\xi}+D\mu\tilde{\xi}-\mathbf{v}\tilde{\xi})=\phi\lambda e^{\mu\cdot\mathbf{y}}\tilde{\xi}\,,\\
&-\nabla\cdot(D\nabla\tilde{\xi}+D\mu\tilde{\xi}-\mathbf{v}\tilde{\xi})-\mu\cdot(D\nabla\tilde{\xi}+D\mu\tilde{\xi}-\mathbf{v}\tilde{\xi})=\phi\lambda\tilde{\xi}\,,\\
&-\nabla\cdot D\nabla\tilde{\xi}-(D\mu-\mathbf{v}+\mu\cdot D)\nabla\tilde{\xi}-\mu\cdot(D\mu-\mathbf{v})\tilde{\xi}=\phi\lambda\tilde{\xi}\,.
\end{aligned}
\tag{22}
$$

Choose μ so that $D\mu+\mu\cdot D=\mathbf{v}$. Then by inserting (21) into (20) we obtain

$$-\nabla\cdot D\nabla\tilde{\xi}+\mu D\mu\tilde{\xi}=\phi\lambda\tilde{\xi}.$$

That is, $\tilde{\xi}(\mathbf{y})$ satisfies the standard *self-adjoint eigenvalue problem*

$$-\nabla\cdot D\nabla\tilde{\xi}+\mu D\mu\tilde{\xi}=\lambda\phi\tilde{\xi}\text{ in }\Omega_{0s},\ \tilde{\xi}=0\text{ on }\Gamma_0. \tag{23}$$

This has eigenfunctions and real positive eigenvalues $\{\tilde{\xi}_i(\mathbf{y}),\ \lambda_i\}$; the eigenfunctions are an orthonormal basis for $L^2(\Omega_{0s})$:

$$\int_{\Omega_{0s}}\tilde{\xi}_i\tilde{\xi}_j\,dy=\delta_{ij},\quad \phi\lambda_i>\mu D\mu\,. \tag{24}$$

It follows that $\{\xi_i(\mathbf{y})=e^{\mu\cdot\mathbf{y}}\tilde{\xi}_i(\mathbf{y})\}$ are the corresponding eigenfunctions for the problem (20), and they are orthonormal in the weighted space,

$$\int_{\Omega_{0s}}\xi_i(\mathbf{y})\xi_j(\mathbf{y})e^{-2\mu\cdot\mathbf{y}}\,dy=\delta_{ij},\quad \phi\lambda_i>\mu D\mu\,. \tag{25}$$

Now, we write the solution of (19) in the form

$$r(\mathbf{y},t)=\sum_{i=1}^{\infty}r_i(t)\,\xi_i(\mathbf{y})$$

and find that necessarily $\phi\dot{r}_i(t)+\phi\lambda_i r_i(t)=0,\ i\geq 1$, so we have

$$r(\mathbf{y},t)=\sum_{i=1}^{\infty}c_i\,e^{-\lambda_i t}\xi_i(\mathbf{y}).$$

The constants are determined by the initial condition in (19), namely,

$$r(\mathbf{y},0)=1=\sum_{i=1}^{\infty}c_i\,\xi_i(\mathbf{y}),$$

so from (25) we obtain

$$c_j=\int_{\Omega_{0s}}\xi_j(\mathbf{z})e^{-2\mu\cdot\mathbf{z}}\,dz=\int_{\Omega_{0s}}\tilde{\xi}_j(\mathbf{z})e^{-\mu\cdot\mathbf{z}}\,dz,\quad j\geq 1. \tag{26}$$

In summary, we have

$$r(\mathbf{y},t)=\sum_{i=1}^{\infty}\int_{\Omega_{0s}}\xi_i(\mathbf{z})e^{-2\mu\cdot\mathbf{z}}\,dz\,e^{-\lambda_i t}\xi_i(\mathbf{y}),$$

or equivalently in terms of the eigenfunctions of (23)

$$r(\mathbf{y},t)=\sum_{i=1}^{\infty}\int_{\Omega_{0s}}\tilde{\xi}_i(\mathbf{z})e^{-\mu\cdot\mathbf{z}}\,dz\,e^{-\lambda_i t}e^{\mu\cdot\mathbf{y}}\tilde{\xi}_i(\mathbf{y}). \tag{27}$$

The original representative solution of (10) is given by

$$r^0(\mathbf{y},t) = \sum_{i=1}^{\infty} \int_{\Omega_{0s}} \xi_i(\mathbf{z}) e^{-2\mu\cdot\mathbf{z}}\, dz\, (1-e^{-\lambda_i t})\xi_i(\mathbf{y})$$

$$= \sum_{i=1}^{\infty} \int_{\Omega_{0s}} \tilde{\xi}_i(\mathbf{z}) e^{-\mu\cdot\mathbf{z}}\, dz\, (1-e^{-\lambda_i t}) e^{\mu\cdot\mathbf{y}} \tilde{\xi}_i(\mathbf{y}). \tag{28}$$

4.2. The affine representatives r^k. It is useful to consider the translated function $r_k(\mathbf{y},t) = (\mathbf{y}-\mathbf{x}_0^c)_k - r^k(\mathbf{y},t)$ which solves the initial-boundary-value problem

$$\begin{cases} \phi \frac{\partial r_k}{\partial t} - \nabla\cdot(D\nabla r_k - \mathbf{v} r_k) & = v_k, & \mathbf{y}\in\Omega_{0s}, \\ r_k(\mathbf{y},0) & = (\mathbf{y}-\mathbf{x}_0^c)_k, & \mathbf{y}\in\Omega_{0s}, \\ r_k(\mathbf{y},t) & = 0, & \mathbf{y}\in\Gamma_0, \end{cases} \tag{29}$$

with homogeneous boundary conditions. As above, we write the solution of (29) in the form

$$r_k(\mathbf{y},t) = \sum_{i=1}^{\infty} r_i^k(t)\, \xi_i(\mathbf{y})$$

and find that necessarily $\phi \dot{r}_i^k(t) + \phi\lambda_i r_i^k(t) = v_k c_i,\ i \ge 1$. The general solution is

$$r_i^k(t) = d_i e^{-\lambda_i t} + \frac{v_k c_i}{\lambda_i \phi}(1-e^{-\lambda_i t}),$$

and so we have

$$r_k(\mathbf{y},t) = \sum_{i=1}^{\infty} d_i\, e^{-\lambda_i t}\xi_i(\mathbf{y}) + \sum_{i=1}^{\infty} \frac{v_k c_i}{\lambda_i\phi}(1-e^{-\lambda_i t})\xi_i(\mathbf{y}). \tag{30}$$

The constants d_i are determined by the initial condition in (29), namely,

$$r_k(\mathbf{y},0) = (\mathbf{y}-\mathbf{x}_0^c)_k = \sum_{i=1}^{\infty} d_i\, \xi_i(\mathbf{y}),$$

so from (25) we obtain

$$d_j = \int_{\Omega_{0s}} \xi_j(\mathbf{z}) e^{-2\mu\cdot\mathbf{z}} (\mathbf{z}-\mathbf{x}_0^c)_k\, dz = \int_{\Omega_{0s}} \tilde{\xi}_j(\mathbf{z}) e^{-\mu\cdot\mathbf{z}} (\mathbf{z}-\mathbf{x}_0^c)_k\, dz, \quad j\ge 1. \tag{31}$$

In summary, we have

$$r_k(\mathbf{y},t) = \sum_{i=1}^{\infty} \int_{\Omega_{0s}} \xi_i(\mathbf{z}) e^{-2\mu\cdot\mathbf{z}} (\mathbf{z}-\mathbf{x}_0^c)_k\, dz\, e^{-\lambda_i t}\xi_i(\mathbf{y}) + \sum_{i=1}^{\infty} \frac{v_k c_i}{\lambda_i\phi}(1-e^{-\lambda_i t})\xi_i(\mathbf{y}),$$

or equivalently in terms of the eigenfunctions of (23),

$$r_k(\mathbf{y},t) = \sum_{i=1}^{\infty} \int_{\Omega_{0s}} \tilde{\xi}_i(\mathbf{z}) e^{-\mu\cdot\mathbf{z}} (\mathbf{z}-\mathbf{x}_0^c)_k\, dz\, e^{-\lambda_i t} e^{\mu\cdot\mathbf{y}} \tilde{\xi}_i(\mathbf{y})$$
$$+ \sum_{i=1}^{\infty} \frac{v_k c_i}{\lambda_i\phi}(1-e^{-\lambda_i t}) e^{\mu\cdot\mathbf{y}} \tilde{\xi}_i(\mathbf{y}).$$

Finally, since $r_k(\mathbf{y},0)=(\mathbf{y}-\mathbf{x}_0^c)_k$, the corresponding representative functions (12) are given by

$$\begin{aligned} r^k(\mathbf{y},t) =& \sum_{i=1}^{\infty}\int_{\Omega_{0s}}\tilde{\xi}_i(\mathbf{z})e^{-\mu\cdot\mathbf{z}}(\mathbf{z}-\mathbf{x}_0^c)_k\,dz\,(1-e^{-\lambda_i t})e^{\mu\cdot\mathbf{y}}\tilde{\xi}_i(\mathbf{y}) \\ &-\sum_{i=1}^{\infty}\frac{v_k c_i}{\lambda_i\phi}(1-e^{-\lambda_i t})e^{\mu\cdot\mathbf{y}}\tilde{\xi}_i(\mathbf{y}) \\ =&\sum_{i=1}^{\infty}\left(\int_{\Omega_{0s}}\tilde{\xi}_i(\mathbf{z})e^{-\mu\cdot\mathbf{z}}(\mathbf{z}-\mathbf{x}_0^c)_k\,dz-\frac{v_k c_i}{\lambda_i\phi}\right)(1-e^{-\lambda_i t})e^{\mu\cdot\mathbf{y}}\tilde{\xi}_i(\mathbf{y}) \\ =&\sum_{i=1}^{\infty}\int_{\Omega_{0s}}\tilde{\xi}_i(\mathbf{z})e^{-\mu\cdot\mathbf{z}}\left((\mathbf{z}-\mathbf{x}_0^c)_k-\frac{v_k}{\lambda_i\phi}\right)dz\,(1-e^{-\lambda_i t})e^{\mu\cdot\mathbf{y}}\tilde{\xi}_i(\mathbf{y}),\ k=1,2. \end{aligned} \tag{32}$$

4.3. The kernels. Now, we can compute the kernels. The first is given by (28)

$$\begin{aligned} \mathcal{T}^{00}(t) &= \frac{1}{|\Omega_0|}\int_{\Omega_{0s}}\phi\frac{\partial r^0(\mathbf{y},t)}{\partial t}dy \\ &= \frac{\phi}{|\Omega_0|}\sum_{i=1}^{\infty}\int_{\Omega_{0s}}\tilde{\xi}_i(\mathbf{z})e^{-\mu\cdot\mathbf{z}}\,dz\int_{\Omega_{0s}}\tilde{\xi}_i(\mathbf{y})\,e^{\mu\cdot\mathbf{y}}\,dy\,\lambda_i\,e^{-\lambda_i t}. \end{aligned} \tag{33}$$

The remaining averages of rate of change in time are given likewise by (32)

$$\begin{aligned} \mathcal{T}^{k0}(t) &\equiv \frac{1}{|\Omega_0|}\int_{\Omega_{0s}}\phi\frac{\partial r^k}{\partial t}(\mathbf{y},t)\,dy \\ &= \frac{\phi}{|\Omega_0|}\sum_{i=1}^{\infty}\left(\int_{\Omega_{0s}}\tilde{\xi}_i(\mathbf{z})e^{-\mu\cdot\mathbf{z}}(\mathbf{z}-\mathbf{x}_0^c)_k\,dz-\frac{v_k c_i}{\lambda_i\phi}\right)(\lambda_i e^{-\lambda_i t})\int_{\Omega_{0s}}e^{\mu\cdot\mathbf{y}}\tilde{\xi}_i(\mathbf{y})\,dy \\ &= \frac{\phi}{|\Omega_0|}\sum_{i=1}^{\infty}\int_{\Omega_{0s}}\tilde{\xi}_i(\mathbf{z})e^{-\mu\cdot\mathbf{z}}\left((\mathbf{z}-\mathbf{x}_0^c)_k-\frac{v_k}{\lambda_i\phi}\right)dz\int_{\Omega_{0s}}e^{\mu\cdot\mathbf{y}}\tilde{\xi}_i(\mathbf{y})\,dy\,(\lambda_i e^{-\lambda_i t}), \\ &\qquad\qquad k=1,2. \end{aligned} \tag{34}$$

Next, the kernels $\mathcal{T}^{k1},\mathcal{T}^{k2}$ arising from the first moments of r^k are given by (28) and (32), respectively, as

$$\begin{aligned} \mathcal{T}^{0j}(t) &\equiv \frac{\phi}{|\Omega_0|}\int_{\Omega_{0s}}\frac{\partial r^0}{\partial t}(\mathbf{y},t)(\mathbf{y}-(\mathbf{x}_0^c))_j\,dy \\ &= \frac{\phi}{|\Omega_0|}\sum_{i=1}^{\infty}\int_{\Omega_{0s}}\tilde{\xi}_i(\mathbf{z})e^{-\mu\cdot\mathbf{z}}\,dz\int_{\Omega_{0s}}\tilde{\xi}_i(\mathbf{y})\,e^{\mu\cdot\mathbf{y}}(\mathbf{y}-(\mathbf{x}_0^c))_j\,dy\,\lambda_i\,e^{-\lambda_i t},\ j=1,2, \end{aligned} \tag{35}$$

$$\begin{aligned} \mathcal{T}^{kj}(t) &\equiv \frac{\phi}{|\Omega_0|}\int_{\Omega_{0s}}\frac{\partial r^k}{\partial t}(\mathbf{y},t)(\mathbf{y}-(\mathbf{x}_0^c))_j\,dy \\ &= \frac{\phi}{|\Omega_0|}\sum_{i=1}^{\infty}\left(\int_{\Omega_{0s}}\tilde{\xi}_i(\mathbf{z})e^{-\mu\cdot\mathbf{z}}(\mathbf{z}-\mathbf{x}_0^c)_k\,dz-\frac{v_k c_i}{\lambda_i\phi}\right)(\lambda_i e^{-\lambda_i t})\int_{\Omega_{0s}}e^{\mu\cdot\mathbf{y}}\tilde{\xi}_i(\mathbf{y})(\mathbf{y}-(\mathbf{x}_0^c))_j\,dy \\ &= \frac{\phi}{|\Omega_0|}\sum_{i=1}^{\infty}\int_{\Omega_{0s}}\tilde{\xi}_i(\mathbf{z})e^{-\mu\cdot\mathbf{z}}\left((\mathbf{z}-\mathbf{x}_0^c)_k-\frac{v_k}{\lambda_i\phi}\right)dz\int_{\Omega_{0s}}e^{\mu\cdot\mathbf{y}}\tilde{\xi}_i(\mathbf{y})(\mathbf{y}-(\mathbf{x}_0^c))_j\,dy\,(\lambda_i e^{-\lambda_i t}). \\ &\qquad\qquad j=1,2,\ k=1,2. \end{aligned} \tag{36}$$

Finally, the *flux kernels* are given by

$$\mathbf{S}^k(t) = (S^{k1}(t), S^{k2}(t)) = \frac{1}{|\Omega_0|}\int_{\Omega_{0s}} (D\nabla r^k(\mathbf{y},t) - \mathbf{v}r^k(\mathbf{y},t))\,dy.$$

The first term can be simplified. For each $k = 0, 1, 2$, we have

$$\int_{\Omega_{0s}} \nabla r^k(\mathbf{y},t)\,dy = \int_{\Gamma_0} \mathbf{n}(\mathbf{y}) r^k(\mathbf{y},t)\,dS_y.$$

For $k = 0$, this is $\int_{\Gamma_0} \mathbf{n}(\mathbf{y})\,dS_y = \int_{\Omega_{0s}} \nabla(1)\,dy = 0$, and for $k = 1, 2$, this is

$$\int_{\Gamma_0} \mathbf{n}(\mathbf{y})(\mathbf{y} - x_0^c)_k\,dS_y = \int_{\Omega_{0s}} \nabla(\mathbf{y} - x_0^c)_k\,dy = |\Omega_{0s}|\mathbf{e}_k.$$

Thus, we have

$$\begin{aligned}\mathbf{S}^0(t) &= -\frac{1}{|\Omega_0|}\int_{\Omega_{0s}} \mathbf{v}r^0(\mathbf{y},t)\,dy \\ &= -\frac{\mathbf{v}}{|\Omega_0|}\sum_{i=1}^{\infty}\int_{\Omega_{0s}} \tilde{\xi}_i(\mathbf{z})e^{-\mu\cdot\mathbf{z}}\,dz \int_{\Omega_{0s}} \tilde{\xi}_i(\mathbf{y})\,e^{\mu\cdot\mathbf{y}}\,dy\,(1 - e^{-\lambda_i t}). \qquad (37)\end{aligned}$$

and for $k = 1, 2$,

$$\begin{aligned}\mathbf{S}^k(t) =& \frac{|\Omega_{0s}|}{|\Omega_0|}D\mathbf{e}_k - \frac{1}{|\Omega_0|}\int_{\Omega_{0s}} \mathbf{v}r^k(\mathbf{y},t)\,dy \\ =& \frac{|\Omega_{0s}|}{|\Omega_0|}D\mathbf{e}_k - \frac{\mathbf{v}}{|\Omega_0|}\sum_{i=1}^{\infty}\int_{\Omega_{0s}} \tilde{\xi}_i(\mathbf{z})e^{-\mu\cdot\mathbf{z}}\left((\mathbf{z} - \mathbf{x}_0^c)_k - \frac{v_k}{\lambda_i\phi}\right)dz \\ &\times \int_{\Omega_{0s}} e^{\mu\cdot\mathbf{y}}\tilde{\xi}_i(\mathbf{y})\,dy\,(1 - e^{-\lambda_i t})\,. \qquad (38)\end{aligned}$$

4.3.1. L^1 estimates. Each of the kernels will be shown to be integrable, and we display the corresponding estimates. The first kernel is estimated by

$$\int_0^\alpha \mathcal{T}^{00}(t)\,dt = \frac{\phi}{|\Omega_0|}\int_{\Omega_{0s}} r^0(\mathbf{y},\alpha)dy \le \frac{\phi|\Omega_{0s}|}{|\Omega_0|}\,, \qquad (39)$$

and the remaining averages are estimated by

$$\int_0^\alpha \mathcal{T}^{k0}(t)\,dt = \frac{\phi}{|\Omega_0|}\int_{\Omega_{0s}} r^k(\mathbf{y},\alpha)\,dy \le \frac{\phi|\Omega_{0s}|}{|\Omega_0|}\sup_{\mathbf{y}\in\Gamma_0}|(\mathbf{y} - \mathbf{x}_0^c)_k|\,, \quad k = 1, 2. \qquad (40)$$

The kernels $\mathcal{T}^{k1}, \mathcal{T}^{k2}$ arising from the first moments of r^k are estimated by

$$\begin{aligned}\int_0^\alpha \mathcal{T}^{0j}(t)\,dt =& \frac{\phi}{|\Omega_0|}\int_{\Omega_{0s}} r^0(\mathbf{y},\alpha)(\mathbf{y} - (\mathbf{x}_0^c))_j\,dy \\ \le& \frac{\phi|\Omega_{0s}|}{|\Omega_0|}\sup_{\mathbf{y}\in\Gamma_0}|(\mathbf{y} - \mathbf{x}_0^c)_j|\,, \quad j = 1, 2, \qquad (41)\end{aligned}$$

$$\begin{aligned}\int_0^\alpha \mathcal{T}^{kj}(t)\,dt =& \frac{\phi}{|\Omega_0|}\int_{\Omega_{0s}} r^k(\mathbf{y},\alpha)(\mathbf{y} - (\mathbf{x}_0^c))_j\,dy \\ \le& \frac{\phi|\Omega_{0s}|}{|\Omega_0|}\sup_{\mathbf{y}\in\Gamma_0}|(\mathbf{y} - \mathbf{x}_0^c)_k|\sup_{\mathbf{y}\in\Gamma_0}|(\mathbf{y} - \mathbf{x}_0^c)_j|\,, \quad j = 1, 2,\ k = 1, 2. \qquad (42)\end{aligned}$$

4.4. An example. Set $\Omega_{0s} = (0,\ell)\times(0,\ell)$ and suppose that D is a diagonal matrix: $D = \left(\begin{smallmatrix} d_1 & 0 \\ 0 & d_2 \end{smallmatrix}\right)$ with $d_1,\ d_2 > 0$. Since μ is determined by $D\mu + \mu\cdot D = \mathbf{v}$, we have $2d_i\mu_i = v_i$ for $i = 1, 2$. To solve the eigenvalue problem (23) we rewrite it as

$$-(d_1\partial_{y_1}^2 + d_2\partial_{y_2}^2)\tilde{\xi} = \beta\tilde{\xi} \text{ in } \Omega_{0s},\ \tilde{\xi} = 0 \text{ on } \partial\Omega_{0s}, \tag{43}$$

and separate variables $\tilde{\xi} = X(y_1)Y(y_2)$ to get

$$-d_1\frac{X''}{X} - d_2\frac{Y''}{Y} = \beta, \quad X(0) = X(\ell) = Y(0) = Y(\ell) = 0.$$

The functions $X_m(y_1) = \sin(\frac{m\pi y_1}{\ell}), Y_n(y_2) = \sin(\frac{n\pi y_2}{\ell})$ give the normalized solutions

$$\begin{aligned} &\tilde{\xi}_{m,n}(y_1,y_2) = (\tfrac{2}{\ell})\sin(\tfrac{m\pi y_1}{\ell})\sin(\tfrac{n\pi y_2}{\ell}), \\ &\beta_{m,n} = d_1(\tfrac{m\pi}{\ell})^2 + d_2(\tfrac{n\pi}{\ell})^2), \quad m,\ n \geq 1. \end{aligned} \tag{44a}$$

These are the eigenfunctions of (23) and the eigenvalues are

$$\lambda_{m,n} = \frac{\mu D\mu}{\phi} + \frac{1}{\phi}\beta_{m,n} = \frac{1}{\phi}(d_1\mu_1^2 + d_2\mu_2^2 + d_1(\tfrac{m\pi}{\ell})^2 + d_2(\tfrac{n\pi}{\ell})^2), \quad m,\ n \geq 1. \tag{44b}$$

4.4.1. The representative functions. Here, we compute explicitly the representative functions $r^0(\mathbf{y},t) =$ (28) and $r^k(\mathbf{y},t) =$ (32) for $k = 1, 2$. We shall use the integration formulae

$$\int e^{au}\sin(bu)du = \frac{e^{au}}{a^2+b^2}(a\sin(bu) - b\cos(bu))$$

and

$$\begin{aligned} &\int (u-c)e^{au}\sin(bu)du \\ =&\frac{u-c}{a^2+b^2}e^{au}(a\sin(bu) - b\cos(bu)) + \frac{1}{(a^2+b^2)^2}e^{au}(2ab\cos(bu) + (b^2-a^2)\sin(bu)). \end{aligned}$$

For the coefficients (26) of the constant representative (28), we compute ($i = [m,n]$)

$$\begin{aligned} &\int_{\Omega_{0s}} \tilde{\xi}_i(\mathbf{z})e^{-\mu\cdot\mathbf{z}}\,dz \\ =&\int_0^\ell\int_0^\ell (\tfrac{2}{\ell})\sin(\tfrac{m\pi y_1}{\ell})\sin(\tfrac{n\pi y_2}{\ell})e^{-(\mu_1 y_1+\mu_2 y_2)}dy_1dy_2 \\ =&\int_0^\ell (\tfrac{2}{\ell})^{\frac{1}{2}}\sin(\tfrac{m\pi y_1}{\ell})e^{-\mu_1 y_1}dy_1 \int_0^\ell (\tfrac{2}{\ell})^{\frac{1}{2}}\sin(\tfrac{n\pi y_2}{\ell})e^{-\mu_2 y_2}dy_2 \\ =&(\frac{2}{\ell})^{\frac{1}{2}}\left[\frac{e^{-\mu_1 y_1}}{\mu_1^2 + (\frac{m\pi}{\ell})^2}(-\mu_1\sin(\tfrac{m\pi y_1}{\ell}) - \tfrac{m\pi}{\ell}\cos(\tfrac{m\pi y_1}{\ell}))\right]_0^\ell \\ &\times(\frac{2}{\ell})^{\frac{1}{2}}\left[\frac{e^{-\mu_2 y_2}}{\mu_2^2 + (\frac{n\pi}{\ell})^2}(-\mu_1\sin(\tfrac{n\pi y_2}{\ell}) - \tfrac{n\pi}{\ell}\cos(\tfrac{n\pi y_2}{\ell}))\right]_0^\ell \\ =&(\tfrac{2}{\ell})^{\frac{1}{2}}\frac{\frac{m\pi}{\ell}}{\mu_1^2 + (\frac{m\pi}{\ell})^2}\left(1 - e^{-\mu_1\ell}\cos(m\pi)\right) \times (\tfrac{2}{\ell})^{\frac{1}{2}}\frac{\frac{n\pi}{\ell}}{\mu_2^2 + (\frac{n\pi}{\ell})^2}\left(1 - e^{-\mu_2\ell}\cos(n\pi)\right) \\ =&(\frac{2}{\ell})\frac{\frac{m\pi}{\ell}}{\mu_1^2 + (\frac{m\pi}{\ell})^2}\cdot\frac{\frac{n\pi}{\ell}}{\mu_2^2 + (\frac{n\pi}{\ell})^2}\left(1 - e^{-\mu_1\ell}\cos(m\pi)\right)\left(1 - e^{-\mu_2\ell}\cos(n\pi)\right). \end{aligned}$$

Note that we have used $\sin(\frac{m\pi y_1}{\ell})|_{y_1=0}^{y_1=\ell} = 0$.

In summary, we have

$$\int_{\Omega_{0s}} \tilde{\xi}_i(\mathbf{z}) e^{-\mu\cdot\mathbf{z}}\, dz = \frac{\ell}{2\ell^4} \frac{2m\pi}{(\mu_1^2 + (\frac{m\pi}{\ell})^2)} \frac{2n\pi}{(\mu_2^2 + (\frac{n\pi}{\ell})^2)} \left(1 - e^{-\mu_1\ell}\cos(m\pi)\right) \times \left(1 - e^{-\mu_2\ell}\cos(n\pi)\right).$$

We shall denote this by

$$\int_{\Omega_{0s}} \tilde{\xi}_i(\mathbf{z}) e^{-\mu\cdot\mathbf{z}}\, dz = a(m,\mu_1)a(n,\mu_2), \tag{45}$$

where we have defined

$$a(m,\mu) \equiv \int_0^\ell (\tfrac{2}{\ell})^{\frac{1}{2}} \sin(\tfrac{m\pi y}{\ell}) e^{-\mu y} dy = \int_0^\ell (\tfrac{2}{\ell})^{\frac{1}{2}} \sin(\tfrac{m\pi y}{\ell}) e^{-\mu y} dy$$
$$= \frac{1}{\ell^2} \frac{\sqrt{2\ell} m\pi}{\mu^2 + (\frac{m\pi}{\ell})^2} \left(1 - e^{-\mu\ell}\cos(m\pi)\right) = \frac{\sqrt{2\ell} m\pi}{(\mu\ell)^2 + (m\pi)^2} \left(1 - e^{-\mu\ell}\cos(m\pi)\right).$$

The original representative solution (28) is finally given by

$$r^0(\mathbf{y},t) = \sum_{i=1}^{\infty} \int_{\Omega_{0s}} \tilde{\xi}_i(\mathbf{z}) e^{-\mu\cdot\mathbf{z}}\, dz\, (1 - e^{-\lambda_i t}) e^{\mu\cdot\mathbf{y}} \tilde{\xi}_i(\mathbf{y}) =$$
$$= \sum_{m\geq 1, n\geq 1} a(m,\mu_1)a(n,\mu_2)\, (1 - e^{-\lambda_{m,n} t}) e^{\mu\cdot\mathbf{y}} \tilde{\xi}_{m,n}(\mathbf{y}). \tag{46}$$

We continue with the coefficients of the affine representative (32) (with $k = 1$) . The first part is

$$\int_{\Omega_{0s}} e^{-\mu\cdot\mathbf{y}} \tilde{\xi}_i(\mathbf{y}) (\mathbf{y} - (\mathbf{x}_0^c))_1\, dy$$
$$= \int_0^\ell \int_0^\ell (\tfrac{2}{\ell}) \sin(\tfrac{m\pi y_1}{\ell}) \sin(\tfrac{n\pi y_2}{\ell}) e^{-(\mu_1 y_1 + \mu_2 y_2)} (y_1 - x_{0,1}^c) dy_1 dy_2$$
$$= \int_0^\ell (\tfrac{2}{\ell})^{\frac{1}{2}} \sin(\tfrac{m\pi y_1}{\ell}) e^{-\mu_1 y_1} (y_1 - x_{0,1}^c) dy_1\, a(n,\mu_2).$$

The second factor is the same as above, but the first factor is given by

$$(\frac{2}{\ell})^{\frac{1}{2}} \big[\frac{(y_1 - x_{0,1}^c)}{\mu_1^2 + (\frac{m\pi}{\ell})^2} e^{-\mu_1 y_1} (-\mu_1 \sin(\tfrac{m\pi y_1}{\ell}) - \tfrac{m\pi}{\ell} \cos(\tfrac{m\pi y_1}{\ell}))$$
$$+ \frac{1}{(\mu_1^2 + (\frac{m\pi}{\ell})^2)^2} e^{-\mu_1 y_1} (-2\mu_1 \tfrac{m\pi}{\ell} \cos(\tfrac{m\pi y_1}{\ell}) + ((\tfrac{m\pi}{\ell})^2 - \mu_1^2) \sin(\tfrac{m\pi y_1}{\ell})) \big]_0^\ell$$
$$= (\frac{2}{\ell})^{\frac{1}{2}} \big[\frac{-\frac{\ell}{2}}{\mu_1^2 + (\frac{m\pi}{\ell})^2} \tfrac{m\pi}{\ell} (1 + e^{-\mu_1\ell}\cos(m\pi)) + \frac{2\mu_1 \frac{m\pi}{\ell}}{(\mu_1^2 + (\frac{m\pi}{\ell})^2)^2} (1 - e^{-\mu_1\ell}\cos(m\pi)) \big]$$
$$= -(\frac{\ell}{2})^{\frac{3}{2}} \frac{2m\pi}{(\mu_1\ell)^2 + (m\pi)^2} (1 + e^{-\mu_1\ell}\cos(m\pi))$$
$$+ (\frac{\ell}{2})^{\frac{1}{2}} \frac{4\mu_1 m\pi\ell^2}{((\mu_1\ell)^2 + (m\pi)^2)^2} (1 - e^{-\mu_1\ell}\cos(m\pi)).$$

We summarize this with our notation above as

$$\begin{aligned}
&\int_{\Omega_{0s}} e^{-\mu\cdot\mathbf{y}}\tilde{\xi}_i(\mathbf{y})(\mathbf{y}-(\mathbf{x}_0^c))_1\,dy\\
=&\tilde{b}(m,\mu_1)\,a(n,\mu_2)\\
=&\left(-\frac{\ell}{2}\tilde{a}(m,\mu_1)+\frac{2\mu_1\ell^2}{(\mu_1\ell)^2+(m\pi)^2}a(m,\mu_1)\right)a(n,\mu_2), \qquad (47)
\end{aligned}$$

where we have additionally defined

$$\begin{aligned}
\tilde{a}(m,\mu) &\equiv \frac{\sqrt{2\ell}m\pi}{(\mu\ell)^2+(m\pi)^2}(1+e^{-\mu\ell}\cos(m\pi)),\\
\tilde{b}(m,\mu) &\equiv -\frac{\ell}{2}\tilde{a}(m,\mu)+\frac{2\mu\ell^2}{(\mu\ell)^2+(m\pi)^2}a(m,\mu).
\end{aligned}$$

The complete expression for the first factor of the coefficients for the affine representative (32) is obtained by subtracting the multiple

$$\frac{\mathbf{v}_1}{\lambda_i\phi}=\frac{2d_1\mu_1}{d_1\mu_1^2+d_2\mu_2^2+d_1(\frac{m\pi}{\ell})^2+d_2(\frac{n\pi}{\ell})^2}$$

of our preceding calculation (45) to get

$$\begin{aligned}
&\int_{\Omega_{0s}}\tilde{\xi}_i(\mathbf{z})e^{-\mu\cdot\mathbf{z}}\left((\mathbf{z}-\mathbf{x}_0^c)_1-\frac{v_1}{\lambda_i\phi}\right)dz\\
=&\left(-\frac{\ell}{2}\tilde{a}(m,\mu_1)+(\frac{2\mu_1\ell^2}{(\mu_1\ell)^2+(m\pi)^2}\right.\\
&\left.-\frac{2d_1\mu_1\ell^2}{d_1(\mu_1\ell)^2+d_2(\mu_2\ell)^2+d_1(m\pi)^2+d_2(n\pi)^2})a(m,\mu_1)\right)a(n,\mu_2)\\
=&b(m,\mu_1)\,a(n,\mu_2), \qquad (48)
\end{aligned}$$

where we have defined

$$\begin{aligned}
b(m,\mu_1)\equiv&-\frac{\ell}{2}\tilde{a}(m,\mu_1)\\
&+\frac{2d_1\mu_1\ell^2((\mu_2\ell)^2+(n\pi)^2)d_2}{d_1((\mu_1\ell)^2+(m\pi)^2)(d_1(\mu_1\ell)^2+d_2(\mu_2\ell)^2+d_1(m\pi)^2+d_2(n\pi)^2)}a(m,\mu_1)\,.
\end{aligned}$$

We also specify the symmetric counterpart

$$\begin{aligned}
b(n,\mu_2)\equiv&-\frac{\ell}{2}\tilde{a}(n,\mu_2)\\
&+\frac{2d_2\mu_2\ell^2((\mu_1\ell)^2+(m\pi)^2)d_1}{d_2((\mu_2\ell)^2+(n\pi)^2)(d_1(\mu_1\ell)^2+d_2(\mu_2\ell)^2+d_1(m\pi)^2+d_2(n\pi)^2)}a(n,\mu_2)\,.
\end{aligned}$$

The affine representative solution (32) is finally given by

$$\begin{aligned}
r^1(\mathbf{y},t)=&\sum_{i=1}^{\infty}\int_{\Omega_{0s}}\tilde{\xi}_i(\mathbf{z})e^{-\mu\cdot\mathbf{z}}\left((\mathbf{z}-\mathbf{x}_0^c)_1-\frac{v_1}{\lambda_i\phi}\right)dz\,(1-e^{-\lambda_i t})e^{\mu\cdot\mathbf{y}}\tilde{\xi}_i(\mathbf{y})\\
=&\sum_{m\geq 1,n\geq 1}b(m,\mu_1)\,a(n,\mu_2)\,(1-e^{-\lambda_{m,n}t})e^{\mu\cdot\mathbf{y}}\tilde{\xi}_{m,n}(\mathbf{y}), \qquad (49)
\end{aligned}$$

for $k = 1$ and similarly for $k = 2$, we have

$$r^2(\mathbf{y},t) = \sum_{i=1}^{\infty} \int_{\Omega_{0s}} \tilde{\xi}_i(\mathbf{z}) e^{-\mu\cdot\mathbf{z}} \left((\mathbf{z}-\mathbf{x}_0^c)_2 - \frac{v_2}{\lambda_i \phi} \right) dz \, (1 - e^{-\lambda_i t}) e^{\mu\cdot\mathbf{y}} \tilde{\xi}_i(\mathbf{y})$$

$$= \sum_{m\geq 1, n\geq 1} a(m,\mu_1)\, b(n,\mu_2)\, (1 - e^{-\lambda_{m,n} t}) e^{\mu\cdot\mathbf{y}} \tilde{\xi}_{m,n}(\mathbf{y}). \tag{50}$$

4.4.2. Summary of the kernels.

$$\mathcal{T}^{00}(t) = \frac{\phi}{|\Omega_0|} \sum_{m\geq 1, n\geq 1} a(m,\mu_1)\, a(n,\mu_2)\, a(m,-\mu_1)\, a(n,-\mu_2)\, \lambda_{m,n} e^{-\lambda_{m,n} t},$$

$$\mathcal{T}^{10}(t) = \frac{\phi}{|\Omega_0|} \sum_{m\geq 1, n\geq 1} b(m,\mu_1)\, a(n,\mu_2)\, a(m,-\mu_1)\, a(n,-\mu_2)\, \lambda_{m,n} e^{-\lambda_{m,n} t},$$

$$\mathcal{T}^{20}(t) = \frac{\phi}{|\Omega_0|} \sum_{m\geq 1, n\geq 1} a(m,\mu_1)\, b(n,\mu_2)\, a(m,-\mu_1)\, a(n,-\mu_2)\, \lambda_{m,n} e^{-\lambda_{m,n} t},$$

$$\mathcal{T}^{01}(t) = \frac{\phi}{|\Omega_0|} \sum_{m\geq 1, n\geq 1} a(m,\mu_1)\, a(n,\mu_2)\, \tilde{b}(m,-\mu_1)\, a(n,-\mu_2)\, \lambda_{m,n} e^{-\lambda_{m,n} t},$$

$$\mathcal{T}^{02}(t) = \frac{\phi}{|\Omega_0|} \sum_{m\geq 1, n\geq 1} a(m,\mu_1)\, a(n,\mu_2)\, a(m,-\mu_1)\, \tilde{b}(n,-\mu_2)\, \lambda_{m,n} e^{-\lambda_{m,n} t},$$

$$\mathcal{T}^{11}(t) = \frac{\phi}{|\Omega_0|} \sum_{m\geq 1, n\geq 1} b(m,\mu_1)\, a(n,\mu_2)\, \tilde{b}(m,-\mu_1)\, a(n,-\mu_2)\, \lambda_{m,n} e^{-\lambda_{m,n} t},$$

$$\mathcal{T}^{12}(t) = \frac{\phi}{|\Omega_0|} \sum_{m\geq 1, n\geq 1} b(m,\mu_1)\, a(n,\mu_2)\, a(m,-\mu_1)\, \tilde{b}(n,-\mu_2)\, \lambda_{m,n} e^{-\lambda_{m,n} t},$$

$$\mathcal{T}^{21}(t) = \frac{\phi}{|\Omega_0|} \sum_{m\geq 1, n\geq 1} a(m,\mu_1)\, b(n,\mu_2)\, \tilde{b}(m,-\mu_1)\, a(n,-\mu_2)\, \lambda_{m,n} e^{-\lambda_{m,n} t},$$

$$\mathcal{T}^{22}(t) = \frac{\phi}{|\Omega_0|} \sum_{m\geq 1, n\geq 1} a(m,\mu_1)\, b(n,\mu_2)\, a(m,-\mu_1)\, \tilde{b}(n,-\mu_2)\, \lambda_{m,n} e^{-\lambda_{m,n} t},$$

$$\mathbf{S}^0(t) = -\frac{\mathbf{v}}{|\Omega_0|} \sum_{m\geq 1, n\geq 1} a(m,\mu_1)\, a(n,\mu_2)\, a(m,-\mu_1)\, a(n,-\mu_2)\, (1 - e^{-\lambda_{m,n} t}),$$

$$\mathbf{S}^1(t) = \frac{|\Omega_{0s}|}{|\Omega_0|} D\mathbf{e}_1 - \frac{\mathbf{v}}{|\Omega_0|} \sum_{m\geq 1, n\geq 1} b(m,\mu_1)\, a(n,\mu_2)\, a(m,-\mu_1)\, a(n,-\mu_2)\, (1 - e^{-\lambda_{m,n} t}),$$

$$\mathbf{S}^2(t) = \frac{|\Omega_{0s}|}{|\Omega_0|} D\mathbf{e}_2 - \frac{\mathbf{v}}{|\Omega_0|} \sum_{m\geq 1, n\geq 1} a(m,\mu_1)\, b(n,\mu_2)\, a(m,-\mu_1)\, a(n,-\mu_2)\, (1 - e^{-\lambda_{m,n} t}).$$

4.4.3. Comments on graphs. The representative functions $r = r^k$ (or their complements, $1 - r$, $(\mathbf{y} - \mathbf{x})_k - r^k$) satisfy the abstract Cauchy problem,

$$\dot{r}(t) + Ar(t) = 0, \; r(0) = r_0 \,,$$

with $Ar = -\nabla \cdot (D\nabla r - \mathbf{v}r) \in V'$ for $r \in V \equiv H_0^1(\Omega_{os})$, so we have $r \in L^2(0,T; H_0^1(\Omega_{os}))$, $\dot{r} \in L^2(0,T; H^{-1}(\Omega_{os}))$, and it follows that $r \in C([0,T]; L^2(\Omega_{os}))$ and $\nabla r \in L^2(0,T; L^2(\Omega_{os}))$. From these observations, it follows that each $\mathcal{T}^{kj} \in$

$L^1(0,T)$ and $S^{kj} \in L^1(0,T)$. If $D = constant$ (as in our example), then $S^{kj} \in C[0,T]$.

The basic kernels $\mathcal{T}^{ij}$ all consist of sums of terms $\lambda_{m,n}e^{-\lambda_{m,n}t}$ which rapidly decrease from a singularity at zero. We showed above and in Section 4.3 that they are integrable at zero. The kernels S^{ij} consist of terms $1-e^{-\lambda_{m,n}t}$ which start at zero and have a relatively steady rise to a constant value. Thus, *all* of these basic kernels are integrable at zero.

Recall that the coefficients of the model equation consist of the combined kernels given by (18). Since the kernels are not spatially dependent, the first is just the *double porosity kernel*, $\mathcal{T}^{00}$.

The *secondary advection kernels* are given by

$$\Xi = (\mathcal{T}^{10}, \mathcal{T}^{20}) - \left((\mathcal{T}^{01}, \mathcal{T}^{02}) + (S^{01}, S^{02})\right).$$

The first two terms will sum approximately to zero (by near anti-symmetry properties of the integrands), so it is essentially a convex combination of terms $(1-e^{-\lambda_{m,n}t})$ with small competing terms near zero. In cases where the first two terms are substantial, we may get negative values at very early times.

The *secondary diffusion kernels* are

$$\Psi = \begin{bmatrix} \mathcal{T}^{11} & \mathcal{T}^{12} \\ \mathcal{T}^{21} & \mathcal{T}^{22} \end{bmatrix} + \begin{bmatrix} S^{11} & S^{12} \\ S^{21} & S^{22} \end{bmatrix}.$$

These consist of sums of respective terms of the form $\lambda_{m,n}e^{-\lambda_{m,n}t}$ and $1-e^{-\lambda_{m,n}t}$. The first accounts for the initial rapid decrease, and the second for the delayed interval of increase to a constant level in the case of Ψ^{11} (with all coefficients positive) and the delayed interval of even more rapid decrease in the case of Ψ^{22} (with the second set of coefficients containing negative terms).

Figure 1 illustrates the double porosity, secondary advection, and secondary diffusion kernels for various $\mathbf{K}_{ratio} \equiv \mathbf{K}_f/\mathbf{K}_s$ values.

5. Numerical approximation and analysis of the upscaled model

In this section, we discuss and analyze the discretization of

$$u_t + vu_x - Du_{xx} + \Upsilon * u_t + \Xi * u_{xt} - \Psi * u_{xxt} = 0, \tag{51a}$$

$$u(x,0) = u_0(x), \tag{51b}$$

where v is assumed to be nonnegative. Note that (51) is a 1d version of the upscaled problem (17) considered in Section 3, with scalar fields Ψ and Ξ.

We implemented several schemes for (17) that share a common element that the memory terms are treated implicitly in time, while the spatial derivatives corresponding to the advection and diffusion are handled in a way optimal for the particular scheme. In this section, however, we consider only an upwind-memory scheme which treats the advection explicitly and diffusion implicitly. We do not report on schemes which treat the advection implicitly. While they can increase the stability of the method, additional numerical diffusion can be introduced.

Below, we first formulate assumptions on the kernels that will be used in our analysis. Then, we define discretization of convolution terms and proceed to define and analyze the schemes corresponding to (51) with increasing level of difficulty.

In order to discretize the memory terms, we use the product integration rule applied in [13] for self-adjoint parabolic equations with memory terms similar to $\Upsilon * u_t$. Recently, in [14], Peszyńska developed schemes for nonlinear conservation laws in which the (possibly nonlinear) advection terms are treated explicitely in

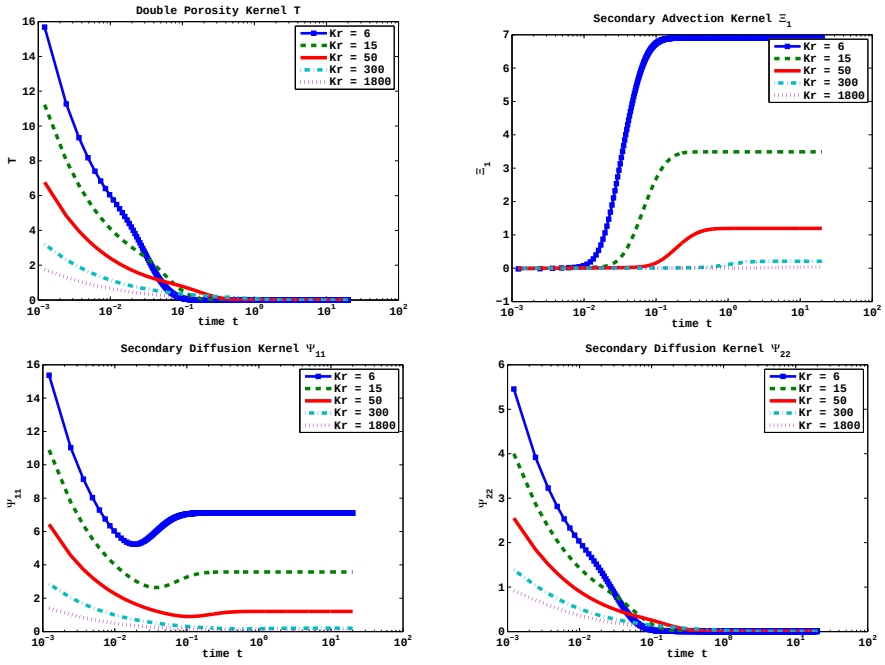

FIGURE 1. Graphs of the kernels, $\mathcal{T}^{00}, \Xi_1$(*top*), and Ψ_{11}, Ψ_{22} (bottom) for various $\mathbf{K}_{ratio}$ values.

time. The theory developed in [14] applies to (51) if $D = 0, \Psi = 0, \Xi = 0$. In this paper, we improve on the strong stability result proved in [14] and extend it to the case when $D \neq 0, \Psi \neq 0, \Xi \neq 0$. Since we are interested in (51) which is linear, we only pursue the linear stability case.

In Section 5.3, we define the general setup of von-Neumann analysis which applies to initial value problems on $\mathbb{R}$. Then, in Sections 5.4–5.7, we use von-Neumann analysis for problems with $\Upsilon \neq 0, \Xi = \Psi = 0$, and $\Upsilon \neq 0, \Xi \neq 0, \Psi = 0$, and finally for $\Upsilon \neq 0, \Xi \neq 0, \Psi \neq 0$. In Section 5.8, we provide discussion of stability using the method of lines (MOL) which applies to initial-boundary value problems.

While we are able to prove weak stability for the comprehensive scheme for (51), this is not optimal since the scheme for the micro-model is strongly stable, reflecting the qualitative properties of the solution subject to maximum principles. Thus, one could expect that the scheme for the limiting macro-model (51) would share the same stability properties. However, we do not make assumptions on the interdependence between the data v and D of the upscaled problem (51) and the kernels Υ, Ξ, and Ψ. Hence, we obtain only weak stability. However, it is possible that one could obtain a stronger result under appropriately stronger hypotheses on v, D, Υ, Ξ, and Ψ. Furthermore, (51) truncates (17) to one dimension. While we are not able to prove a stability result for (17) at this time, it is possible that, unlike (51), it would have strong stability.

Finally, we remark that our analysis assumes only that Ξ and Ψ are both piecewise monotone and bounded as $t \to \infty$. This assumption is justifiable by Section 4. On the other hand, we do not assume boundedness of Υ or of Ψ at 0, but rather allow for their weak singularity at the origin. One can easily extend our results and see that strong stability will hold for convolution terms with any monotonically

decreasing kernels that are weakly singular at $t = 0$ and that weak stability can be obtained for increasing but asymptotically bounded kernels.

To close this preliminary discussion, we mention that it is expensive to keep all the long-term history of the evolution of the solution, *i.e.*, the values u_m. To rectify this problem, one can take advantage of the behavior of the kernels which seem to asymptotically stabilize as discussed below in Remark 4. Thus, a truncation of the scheme proposed here makes sense, but we will not deal with it in this paper.

5.1. Kernels. The kernels Υ and Ξ in (51) will be assumed to be smooth and weakly integrable. Also, both Υ and Ξ are assumed to be monotone, but the former is nonincreasing, whereas the latter is nondecreasing. More specifically,

$$\Upsilon \in L^1_{loc}(0,\infty) \cap C^1(0,\infty), \Upsilon(t) \geq 0,\ \Upsilon'(t) \leq 0,\ \forall t > 0, \tag{52}$$

$$\Xi \in L^1_{loc}(0,\infty) \cap C^1(0,\infty), \Xi(t) \geq 0,\ \Xi'(t) \geq 0,\ \forall t > 0. \tag{53}$$

In addition, we assume

$$\Xi(0) = 0. \tag{54}$$

These assumptions on Ξ are somewhat inconsistent with the comment on the possible negative values of Ξ at very early times in Section 4.4.3. However, the magnitude of $\Xi(t)$ tends to be really small, if not zero, at very early times. Moreover, these assumptions make our analysis much simpler.

Indeed, Ξ has a stronger property of than that in (53). That is,

$$\Xi \in C^0([0,\infty)),$$

but we will not take advantage of this in our analysis.

On the other hand, Ψ is only piecewise monotone: there is a time $t_* > 0$ such that Ψ is nonincreasing on $(0, t_*)$ and nondecreasing on (t_*, ∞):

$$\begin{aligned} &\Psi \in L^1_{loc}(0,\infty) \cap C^1(0,\infty), \Psi(t) \geq 0,\ \forall t > 0, \\ &\Psi'(t) \leq 0,\ \forall t \leq t_*, \Psi'(t) \geq 0,\ \forall t \geq t_*. \end{aligned} \tag{55}$$

Furthermore, we note that there is another time $t^* > t_*$ after which it makes sense to approximate

$$\Upsilon'(t) \approx 0,\ \Xi'(t) \approx 0, \Psi'(t) \approx 0,\ \ t > t^*. \tag{56}$$

5.2. Discretization of convolution terms. In this section, we consider memory terms of the form $\Upsilon * u$ and $\Upsilon * u_t$, for which we temporarily assume $u = u(t)$ and drop the spatial dependence of u for exposition's sake.

The approximations to $\Upsilon * u$ and $\Upsilon * u_t$ depend on the qualitative properties of Υ and possibly on whether, e.g., $u(t)$ is approximated with a piecewise constant, linear, or a higher order polynomial on each time interval $[t_m, t_{m+1}]$. First, we consider approximations to $\Upsilon * u$. Since

$$\Upsilon * u|_{t=t_n} = \int_0^{t_n} \Upsilon(t_n - s)u(s)ds = \sum_{m=0}^{n-1} \int_{t_m}^{t_{m+1}} \Upsilon(t_n - s)u(s)ds,$$

we need to decide how to approximate the integral $I_{n,m} := \int_{t_m}^{t_{m+1}} \Upsilon(t_n - s)u(s)ds$.

Define

$$\Upsilon_m := \frac{1}{k}\int_{t_m}^{t_{m+1}} \Upsilon(s)ds,\ \ \tau_m := k\Upsilon_m = \int_{t_m}^{t_{m+1}} \Upsilon(s)ds. \tag{57}$$

Note that Υ_m is the exact mean value of Υ on $[t_m, t_{m+1}]$, and Υ_m and τ_m are well defined for both bounded and weakly singular kernels. For bounded kernels, the following approximations can also be considered:

$$\Upsilon_m^l := \Upsilon(t_m), \qquad \tau_m^l := k\Upsilon(t_m), \tag{58}$$

$$\Upsilon_m^r := \Upsilon(t_{m+1}), \qquad \tau_m^r := k\Upsilon(t_{m+1}). \tag{59}$$

One could also consider the midpoint formula, but it will not be pursued any further here.

Assume for simplicity a uniform time-stepping with the timestep size k, i.e.,

$$t_m = mk,\ m = 0, 1, \dots.$$

Then, changing variables gives us

$$\int_{t_m}^{t_{m+1}} \Upsilon(t_n - s)ds = \int_{t_n - t_{m+1}}^{t_n - t_m} \Upsilon(s)ds = \int_{t_{n-m-1}}^{t_{n-m}} \Upsilon(s)ds = \tau_{n-m-1}. \tag{60}$$

Now, we introduce the following approximations to $I_{n,m}$:

$$I_{n,m} \approx u_{m+1}\tau_{n-m-1}, \tag{61}$$

$$I_{n,m} \approx u_m\tau_{n-m-1}, \tag{62}$$

$$I_{n,m} \approx u_m\tau^l_{n-m-1}, \tag{63}$$

$$I_{n,m} \approx u_{m+1}\tau^r_{n-m-1}, \tag{64}$$

where u_m is the approximate to $u(mk)$, $m = 1, 2, \cdots$. The formulas (61) and (62) come from the product integration rules and (63) and (64) come from the left- and right- rectangle rules. Also, they are $O(k)$-accurate methods. The rules (61) and (64) lead to a fully implicit treatment of (51), whereas (62) and (63) lead to a fully explicit method. A generic approximation to the convolution integral which allows the implicit and explicit treatments can be written as

$$\Upsilon * u|_{t=t_n} = \sum_{m=0}^{n} \bar{\tau}_{n-m}u_m,$$

where $\bar{\tau}_{n-m}$ can be chosen from (61)–(64) and is set to 0 at $m = 0$ for implicit schemes or at $m = n$ for explicit schemes. In this paper, we consider only implicit treatments.

Next, we define an approximation to $\Upsilon * u_t$ using (57) and (60) as follows:

$$\begin{aligned}
\Upsilon * u_t|_{t=t_n} &= \sum_{m=1}^{n} \int_{t_{m-1}}^{t_m} \Upsilon(t_n - s)u_t(s)ds \\
&\approx \sum_{m=1}^{n}) \frac{1}{k}(u_m - u_{m-1}) \int_{t_{m-1}}^{t_m} \Upsilon(t_n - s)ds \\
&= \sum_{m=1}^{n} \frac{u_m - u_{m-1}}{k}\tau_{n-m}. \qquad (65)
\end{aligned}$$

For bounded kernels, one could also consider approximations (58) or (59) to replace τ_{n-m}.

Remark 1. *The qualitative properties of the sequence Υ_m and those of $\tau_m := k\Upsilon_m$ are inherited from those of the kernel Υ. In particular, we have by* (52) *that Υ is nonnegative and nonincreasing, and so are the sequences $(\Upsilon_m)_m$ and $(\tau_m)_m$, i.e.,*

$$\tau_m \geq 0, \ \ \tau_m - \tau_{m+1} \geq 0, \ \ \forall m. \tag{66}$$

Next, we define Ξ_m, ξ_m and Ψ_m, ψ_m for the kernels Ξ and Ψ, respectively, analogously to (57).

Remark 2. *By* (53)*,* Ξ *is nonnegative and nondecreasing, and so are the sequences* $(\Xi_m)_m$ *and* $(\xi_m)_m$*. More specifically,*

$$0 \le \xi_m \le \xi_{m+1} \le k\Xi(t_{m+2}) \le k\Xi(T),\ \forall m. \tag{67}$$

In Method of Lines analysis, it will be convenient to assume $\xi_0 = 0$ *which amounts to replacing* ξ_0 *by its approximation* ξ_0^l*, which is* 0 *if* (54) *holds.*

Remark 3. *By* (55)*,* Ψ *is nonnegative, and so are the sequences* $(\Psi_m)_m$ *and* $(\psi_m)_m$*. However,* Ψ *is not monotone. Without loss of generality, we assume that* t_* *and* t^* *coincide with some discrete time* t_m*. That is,* $t_* = t_{m_*}$ *and* $t^* = t_{m^*}$ *for some* m_* *and* m^**. Thus, we have*

$$\psi_m \ge 0,\ \psi_m \ge \psi_{m+1},\ m < m_* - 1, \tag{68a}$$

$$\psi_m \ge 0,\ \psi_m \le \psi_{m+1},\ m \ge m_*. \tag{68b}$$

For $m = m^*$*, the sign of* $\psi_{m_*-1} - \psi_{m_*}$ *is in general undecided. Without loss of generality, we assume further*

$$\psi_m \ge 0,\ \psi_m \le \psi_{m+1},\ m = m_* - 1. \tag{68c}$$

Remark 4. *The fact that for* $t > t_{m^*}$ *the derivatives of the kernels* Υ, Ξ, Ψ *appear to vanish suggests to truncate the approximation to the memory terms to only those time steps reaching to* m^**. While we do not analyze the consequences of this truncation, it is an important practical simplification.*

5.3. Stability analysis for $\Upsilon = \Xi = \Psi = 0$. One-level scheme for (51) with $\Upsilon = \Xi = \Psi \equiv 0$ defines u_{n+1} in terms of u_n, $n = 1, 2, \ldots$. More specifically, we have

$$u_{n+1} = C(k)u_n. \tag{69}$$

Here, $u_n = (u_{j,n})_{j\in J}$ is a vector of nodal values at the nodes $x_j = jh$ of the spatial grid and $C(k)$ is a coefficient matrix depending only on the time step k and the original (homogeneous) partial differential equation (PDE). In particular, $C(k)$ reflects how we treat the advection and diffusion terms.

In error analysis of (69), one considers an inhomogeneous version of (69) that allows to account for, e.g., truncation errors in the following form:

$$u_{n+1} = C(k)u_n + kf_n. \tag{70}$$

In fact, this equation holds for the vector of errors e_n. If we apply this recursively, we obtain, with $C = C(k)$,

$$e_{n+1} = C\left(Ce_{n-1} + kf_{n-1}\right) + kf_n = \ldots = C^{n+1}e^0 + k\sum_{m=0}^{n} C^{n-m}f_m. \tag{71}$$

It is clear that to keep the error bounded, one has to keep the growth of C^n under control, i.e, require its uniform boundedness. To analyze the stability of the numerical method, we will use the von Neumann approach, which is based on Fourier analysis. To avoid the details of handling boundary conditions in the von Neumann analysis, one usually studies the stability for the Cauchy problem, which is the PDE on all space with no boundaries, $-\infty < x < \infty$. In this case, $j = 0, \pm 1, \pm 2, \ldots$. For initial boundary value problems on a bounded domain, J is a finite set and we will discuss this case later in Section 5.8.

First, we recall the well-known von-Neumann ansatz that will be fundamental for the understanding of what we develop for the memory terms. Consider the following Fourier series for $u_{j,n}$:

$$u_{j,n} = \sum_{\chi} q_n(\chi) e^{i\chi jh},\ n = 1, 2, \ldots. \tag{72}$$

Here, the coefficient $q_n(\chi)$ is the Fourier mode of the finite difference solution u_n and $q(\chi, t_n)$ is the Fourier coefficient of $u(x, t_n)$. Therefore, $q_n(\chi)$ is an approximation to $q(\chi, t_n)$. In particular, $q_0(\chi)$ is an approximation to $q(\chi, 0) = \frac{1}{2\pi}\int_{-\pi}^{\pi} u(x,0)e^{-i\chi x}dx$, the Fourier coefficients of the initial data $u_0 \approx u(x, 0)$.

Substituting (72) in the difference equation (69) for u_{n+1} and u_n and collecting like terms of $e^{i\chi jh}$, we can identify, at every step n, the same factor $g = g(k, \chi)$ so that

$$q_{n+1}(\chi) = g(k, \chi) q_n(\chi).$$

Applying the above equation recursively, we obtain $q_n(\chi) = g(k, \chi)^n q_0(\chi)$. Then, a better-known version of (72) is

$$u_{j,n} = \sum_{\chi} q_0(\chi) g(k, \chi)^n e^{i\chi jh}. \tag{73}$$

The amplification factor $g(k, \chi)$ is thus the counterpart of $C(k)$ in the Fourier space. In the von Neumann analysis, the following is required for the strong stability:

$$|g(k, \chi)| \le 1,\ \forall \chi. \tag{74}$$

On the other hand, weak stability [[17], *Chapter IV*] relaxes (74) and requires only

$$|g(k, \chi)| \le 1 + O(k),\ \forall \chi. \tag{75}$$

5.4. Strong stability for $\Upsilon \neq 0, \Psi \equiv 0, \Xi \equiv 0$. In this section, we consider

$$u_t + \Upsilon * u_t + v u_x - D u_{xx} = 0. \tag{76}$$

First, we will consider the above model with no diffusion term, *i.e.*, $D = 0$. Then, we will extend our stability analysis to the case with nonzero diffusion term.

5.5. The case of $D = 0$. Consider

$$u_t + \Upsilon * u_t + v u_x = 0. \tag{77}$$

In [14], Peszyńska proposed the following explicit upwind-memory scheme

$$(u_{j,n} - u_{j,n-1}) + \sum_{m=1}^{n} (u_{j,m} - u_{j,m-1})\tau_{n-m} + \lambda v (u_{j,n-1} - u_{j-1,n-1}) = 0, \tag{78}$$

where $\lambda = k/h$. It arose from a standard upwind discretization combined with the approximation (65) for $\Upsilon * u_t$. Following Section 5.3, we can pursue Fourier analysis of this problem and analyze the growth of $q_n(\chi)$, the Fourier mode of the finite difference approximation to u_n. Indeed, Peszyńska pursued the analysis of the amplification factor g in the (pessimistic) case when $q_n = g q_{n-1}$, where g does not depend on n. In this case, at $t = t_n$, it was shown that g is the root of a polynomial equation of order $n + 1$ and its magnitude was estimated using a corollary to Rouche's theorem. It was found that if the following CFL-τ condition

$$0 \le \lambda v \le 1 + \tau_0 \tag{79}$$

is satisfied, we have $|g| \le 1$, which implies strong stability, i.e., $|q_n(\chi)| \le |q_0(\chi)|$.

In this paper, we prove a more general result in which the amplification sequence g_n is defined by

$$q_n(\chi) = g_n(\chi) q_0(\chi) \tag{80}$$

and g_n varies from one time step to another.

The following auxiliary result is elementary in stability analysis [8] and we recall it for later use.

Lemma 5.1. *Assume $A \in \mathbb{R}$. In order for*

$$|1 - A(1 - e^{-i\theta})| \leq 1 \tag{81}$$

to hold for any θ, it is sufficient and necessary to have $0 \leq A \leq 1$.

The proof of Lemma 5.1 is an exercise: we calculate the square of the quantity on the left, and obtain, after some algebraic manipulations, that (81) is equivalent to

$$1 + 2(A^2 - A)(1 - \cos(\theta)) \leq 1.$$

From this, it further follows that we must have $A^2 - A \leq 0$ and the lemma is proved.

Proposition 5.1. *Assume that Υ satisfies* (52)*. Then, the explicit upwind-memory scheme,* (78)*, is strongly stable, i.e.,*

$$|g_n| \leq 1, \ \ \forall \chi, \ n = 1, 2, \ldots, \tag{82}$$

provided the CFL condition

$$0 \leq v\lambda \leq 1 \tag{83}$$

holds.

Proof. First, we recall that, by Lemma 5.1 with $A = v\lambda$, the CFL condition, (83), is equivalent to

$$|1 - \gamma^*| \leq 1, \tag{84}$$

where

$$\gamma^* := v\lambda(1 - z), \ \ z := e^{-i\theta}. \tag{85}$$

Then, the proof of (82) follows by induction. We substitute (72) in (78) and consider the growth of the sequence $|g_n|$, $n = 1, 2, \ldots$.

In what follows, we set $\theta = \chi j h$ to be an arbitrary angle.

1^0: When $n = 1$, (65) gives us

$$(\Upsilon * u_t)|_{x=x_j, t=t_1} \approx \frac{1}{k}(u_{j,1} - u_{j,0})\tau_0.$$

Thus, rewriting (78) upon (72) for $n = 1$, we have, after collecting the like powers of $e^{i\theta}$,

$$(1 + \tau_0)(q_1 - q_0) + q_0\gamma^* = 0. \tag{86}$$

where γ^* arises from the upwind discretization of the advection term vu_x. Using (80) to define g_1 , we see that

$$(1 + \tau_0)g_1 = (1 + \tau_0 - \gamma^*), \tag{87}$$

thus, by recalling $\tau_0 \geq 0$ from (52),

$$(1 + \tau_0)|g_1| = |1 + \tau_0 - \gamma^*|. \tag{88}$$

On the other hand, using $\tau_0 \geq 0$ and (84), we can see that the right hand side of (88) satisfies

$$|1 + \tau_0 - \gamma^*| \leq |1 - \gamma^*| + \tau_0 \leq 1 + \tau_0.$$

Thus, we obtain

$$|g_1| \leq 1. \tag{89}$$

Alternatively, applying Lemma 5.1, we see that $0 \leq A := \frac{v\lambda}{1+\tau_0} \leq 1$ is required to show (89), thus only the CFL-τ condition is needed. In fact, this alternative path can be followed with a possibly negative τ_0, as long as $1 + \tau_0 \geq 0$. Fo a negative τ_0, however, the CFL-τ condition is a more stringent assumption than the CFL condition. However, if $\tau_0 \geq 0$, (83) obviously suffices for the CFL-τ condition.

2^0: Now, consider $n > 1$ and assume $|g_j| \leq 1, j = 1, \dots n-1$. We will prove (82). First, we rewrite (65) to get, for $n > 1$,

$$\begin{aligned}
(\Upsilon * u_t)|_{x=x_j,t=t_n} \approx & \frac{1}{k}[(u_{j,1} - u_{j,0})\tau_{n-1} + (u_{j,2} - u_{j,1})\tau_{n-2} + \dots \\
& + (u_{j,n-1} - u_{j,n-2})\tau_1 + (u_{j,n} - u_{j,n-1})\tau_0] \\
= & \frac{1}{k}[\tau_0 u_{j,n} + (\tau_1 - \tau_0)u_{j,n-1} + (\tau_2 - \tau_1)u_{j,n-2} + \dots \\
& + (\tau_{n-1} - \tau_{n-2})u_{j,1} - \tau_{n-1}u_{j,0}] \\
= & \frac{1}{k}\Big[\tau_0 u_{j,n} + (\tau_1 - \tau_0)u_{j,n-1} \\
& + \sum_{m=1}^{n-2} u_{j,m}(\tau_{n-m} - \tau_{n-m-1}) - u_{j,0}\tau_{n-1}\Big]. \qquad (90)
\end{aligned}$$

Thus, we can rearrange the terms in (78) to get

$$\begin{aligned}
(1 + \tau_0)(u_{j,n} - u_{j,n-1}) + \left[\tau_1 u_{j,n-1} + \sum_{m=1}^{n-2} u_{j,m}(\tau_{n-m} - \tau_{n-m-1}) - u_{j,0}\tau_{n-1}\right] \\
+ v\lambda(u_{j,n-1} - u_{j-1,n-1}) = 0. \qquad (91)
\end{aligned}$$

Then, substituting the Ansatz (72) in (90), setting for convenience $g_0 = 1$, and collecting the like terms e^{ijh}, we obtain an equation for g_n:

$$(1+\tau_0)(g_n - g_{n-1}) + \left[\tau_1 g_{n-1} + \sum_{m=1}^{n-2} g_m(\tau_{n-m} - \tau_{n-m-1}) - g_0\tau_{n-1}\right] + g_{n-1}\gamma^* = 0. \tag{92}$$

Next, we rearrange

$$(1 + \tau_0)g_n = (1 + \tau_0 - \tau_1 - \gamma^*)g_{n-1} - \sum_{m=1}^{n-2} g_m(\tau_{n-m} - \tau_{n-m-1}) + g_0\tau_{n-1}. \tag{93}$$

We then take modulus of both sides and estimate the right hand side by applying the triangle inequality repeatedly. From the inductive assumption, each

$|g_j| \le 1, j = 1, \dots n-1$. Therefore, since τ_m are nonnegative, we have

$$\begin{aligned}(1+\tau_0)|g_n| \le & |1+\tau_0-\tau_1-\gamma^*||g_{n-1}| \\ & + \sum_{m=1}^{n-2} |g_m||\tau_{n-m}-\tau_{n-m-1}| + |g_0|\tau_{n-1} \\ \le & |1-\gamma^*| + |\tau_0-\tau_1| + |\tau_{n-1}-\tau_{n-2}| + |\tau_{n-2}-\tau_{n-3}| + \dots \\ & + |\tau_2-\tau_1| + |\tau_{n-1}|. \end{aligned} \tag{94}$$

Now, by (66), we can replace $|\tau_{n-1}-\tau_{n-2}| = -(\tau_{n-1}-\tau_{n-2})$, etc. in (94) and simplify the expression to obtain

$$\begin{aligned}(1+\tau_0)|g_n| \le & |1-\gamma^*| + \tau_0 - \tau_1 - (\tau_{n-1}-\tau_{n-2}) - (\tau_{n-2}-\tau_{n-3}) - \dots \\ & - (\tau_2-\tau_1) + \tau_{n-1} \\ = & |1-\gamma^*| + \tau_0. \end{aligned} \tag{95}$$

Then, $|g_n| \le 1$ follows from (84).

□

5.5.1. The case of $D \neq 0$. Now, consider

$$u_t + \Upsilon * u_t + v u_x - D u_{xx} = 0. \tag{96}$$

Then, an extension of the explicit upwind-memory scheme discussed in Section 5.3 to (96) is given as follows:

$$\begin{aligned}(u_{j,n}-u_{j,n-1}) + \sum_{m=1}^{n} (u_{j,m}-u_{j,m-1})\tau_{n-m} + \lambda v(u_{j,n-1}-u_{j-1,n-1}) \\ + D\frac{\lambda}{h}(2u_{j,n}-u_{j-1,n}-u_{j+1,n}) = 0, \end{aligned} \tag{97}$$

in which the diffusion term is treated implicitly.

Straightforward modification of the calculations in the proof of Proposition 5.1 reveals that g_1 satisfies, instead of (87),

$$(1+D_h+\tau_0)g_1 = (1+\tau_0-\gamma^*), \tag{98}$$

where $D_h = 2D(1-\cos\theta)\frac{\lambda}{h}$. Since $D_h \ge 0$, we obtain (89).

Proceeding similarly as in the proof of Proposition 5.1 for $n > 1$, we get the modification of (95):

$$\begin{aligned}& (1+D_h+\tau_0)|g_n| \\ \le & |1-\gamma^*| + \tau_0 - \tau_1 - (\tau_{n-1}-\tau_{n-2}) - (\tau_{n-2}-\tau_{n-3}) - \dots - (\tau_2-\tau_1) + \tau_{n-1} \\ = & |1-\gamma^*| + \tau_0. \end{aligned}$$

This proves the induction step and that $|g_n| \le 1$, $n = 1, 2, \dots$.

Corollary 5.1. *Let the assumptions of Proposition 5.1 be satisfied.*
(a) If $v \neq 0$, then the scheme (97) *is strongly stable as long as the CFL condition,* (83)*, holds.*
(b) If $v = 0$, then the scheme (97) *is unconditionally strongly stable. This provides an alternative proof of the result considered in* [13].

5.6. Weak stability for $\Upsilon \neq 0, \Psi \equiv 0, \Xi \not\equiv 0$. Now, consider the following model with a secondary advection term, $\Xi * u_{tx}$:

$$u_t + \Upsilon * u_t + \Xi * u_{tx} + v u_x - D u_{xx} = 0. \tag{99}$$

We approximate $\Xi * u_{tx}$ in analogy to (65), with the upwind discretization for the spatial derivative since Ξ is nonnegative:

$$\Xi * u_{tx}|_{x_j,t_n} \approx \sum_{m=1}^{n} \frac{1}{h} \left((u_{j,m} - u_{j,m-1}) - (u_{j-1,m} - u_{j-1,m-1}) \right) \xi_{n-m}.$$

With this, the scheme for (99) is

$$\begin{aligned} (u_{j,n} - u_{j,n-1}) + \sum_{m=1}^{n} (u_{j,m} - u_{j,m-1}) \tau_{n-m} \\ + \sum_{m=1}^{n} \lambda \left((u_{j,m} - u_{j,m-1}) - (u_{j-1,m} - u_{j-1,m-1}) \right) \xi_{n-m} + \lambda v (u_{j,n-1} - u_{j-1,n-1}) \\ + D \frac{\lambda}{h} (2u_{j,n} - u_{j-1,n} - u_{j+1,n}) = 0. \end{aligned} \tag{100}$$

We will analyze its stability similarly as was done in the proof of Proposition 5.1. For simplicity, we drop temporarily the diffusion terms as we have seen that the inclusion of the diffusion term requires only a minor change in the proof. Thus, in what follows, we set $D = 0$.

First, we consider the difference equation (100) with $D = 0$ for $n = 1$. Using the same von-Neumann framework as in what led to (86), we obtain

$$(1 + \tau_0 + \xi_0^*)(q_1 - q_0) + q_0 \gamma^* = 0, \tag{101}$$

where γ^* and z are the same as in (85) and

$$\xi_m^* := \xi_m \lambda (1 - z), \ m = 0, 1, \ldots. \tag{102}$$

A simple calculation shows that

$$|g_1| = \frac{|1 + \tau_0 + \xi_0^* - \gamma^*|}{|1 + \tau_0 + \xi_o^*|} = \frac{|1 + \tau_0 + \lambda(\xi_0 - v)(1 - z)|}{|1 + \tau_0 + \lambda \xi_0 (1 - z)|}. \tag{103}$$

The following Lemma proves $|g_1| \leq 1$ and also establishes another inequality that will be useful later.

Lemma 5.2. *(i) If the CFL-τ condition,* (79)*, holds, we have*

$$|g_1| \leq 1.$$

(ii) In addition,

$$|1 + \tau_0 + \xi_0^*| = |1 + \tau_0 + \lambda \xi_0 (1 - z)| \geq 1 + \tau_0 \geq 1. \tag{104}$$

Proof. Set $A = 1 + \tau_0$, $B = \lambda(\xi_0 - v)$, and $B_0 = \lambda \xi_0$ and rewrite (103) to obtain

$$|g_1| = \frac{|A + B(1 - z)|}{|A + B_0(1 - z)|} = \frac{|A + B(1 - \cos\theta) + iB \sin\theta|}{|A + B_0(1 - \cos\theta) + iB_0 \sin\theta|}.$$

Then, we compare the (square of the) moduli of the numerator and denominator. To ensure that the former is less than or equal to the latter, we must have

$$A^2 + 2(AB + B^2)(1 - \cos\theta) \leq A^2 + 2(AB_0 + B_0^2)(1 - \cos\theta), \tag{105}$$

which is equivalent to

$$A(B - B_0) \leq (B_0 - B)(B_0 + B).$$

Note that $\xi_0 \geq 0$ gives $B \leq B_0$. Therefore, we have

$$-A \leq B_0 + B = \lambda(2\xi_0 - v). \tag{106}$$

On the other hand, $A \geq 1 > 0$ by definition. Thus, if the right hand side of (106) is positive, the inequality (106) is obviously satisfied. However, the right hand side can be negative asymptotically, since $v \geq 0$ is the data for the problem and $\xi_0 = k\Xi_0 \to 0$ with $k \to 0$. Indeed, we have

$$A \geq v\lambda \geq \lambda(v - 2\xi_0), \tag{107}$$

where the first inequality is due to (79). Hence, the proof of (i) is complete.

To show (ii), we consider the minimum of the quantity $|A + B_0(1-z)|$ on the left hand side of (104) over B_0. Note that its square is the same as the right hand side of (105). For a fixed θ, since $B_0 \geq 0$, the minimum occurs at $B_0 = 0$ and equals A^2, thus (ii) is established. □

Next, we proceed with analysis of the steps for $n > 1$. In this case, it will be shown that, unlike in Proposition 5.1, we do not have strong stability. The von-Neumann Ansatz applied to (100) gives us a modification of the formula (92), defining the amplification sequence g_n, that replaces each occurrence of τ_m in (92) by $\tau_m + \xi_m^*$. First, we write the analogue of (92) as follows:

$$\begin{aligned}(1 + \tau_0 + \xi_0^*)(g_n - g_{n-1}) + \Big[g_{n-1}(\tau_1 + \xi_1^*) + \sum_{m=1}^{n-2} g_m(\tau_{n-m} - \tau_{n-m-1} \\ + \xi_{n-m}^* - \xi_{n-m-1}^*) - g_0(\tau_{n-1} + \xi_{n-1}^*)\Big] + g_{n-1}\gamma^* = 0.\end{aligned} \tag{108}$$

Next, we rearrange the terms by grouping together the expressions involving τ_m and those involving $|\xi_m^*| = \xi_m\lambda|1 - z|$ and estimate similarly as in (94) to see

$$\begin{aligned}|1+\tau_0+\xi_0^*||g_n| \leq (|1-\gamma^*|+|\tau_0-\tau_1|)|g_{n-1}|+\sum_{m=1}^{n-2}|g_m||\tau_{n-m}-\tau_{n-m-1}|+|g_0|\tau_{n-1} \\ + |\xi_0^* - \xi_1^*||g_{n-1}| + \sum_{m=1}^{n-2}|g_m||\xi_{n-m}^* - \xi_{n-m-1}^*| + |g_0||\xi_{n-1}^*|.\end{aligned} \tag{109}$$

Here, we do not invoke the inductive assumption as was done in the proof of Proposition 5.1. Rather, we define $G_{n-1} := \max_{m=0,\ldots n-1}|g_m|$ and use $|g_m| \leq G_{n-1}$ for $m = 0, 1, \ldots n-1$ to estimate the right hand side of (109). Also, we use the monotonicity of τ_m and ξ_m, which allows to cancel some terms. Furthermore, we

accommodate the fact that ξ_m is nondecreasing. Then, we obtain

(110)

$$\begin{aligned}
&|1+\tau_0+\xi_o^*||g_n| \\
&\le G_{n-1}\{|1-\gamma^*| \\
&\quad + (\tau_0-\tau_1)-(\tau_{n-1}-\tau_{n-2})-(\tau_{n-2}-\tau_{n-3})-\ldots-(\tau_2-\tau_1)+\tau_{n-1} \\
&\quad + |\xi_0^*-\xi_1^*|+|\xi_{n-1}^*-\xi_{n-2}^*|+|\xi_{n-2}^*-\xi_{n-3}^*|+\ldots+|\xi_2^*-\xi_1^*|+|\xi_{n-1}^*|\big\} \\
&= G_{n-1}\{|1-\gamma^*|+\tau_0 \\
&\quad + \lambda|1-z|\,(\xi_1-\xi_0+\xi_{n-1}-\xi_{n-2}+\xi_{n-2}-\xi_{n-3}+\ldots+\xi_2-\xi_1+\xi_{n-1})\} \\
&= G_{n-1}(|1-\gamma^*|+\tau_0+\lambda|1-z|(2\xi_{n-1}-\xi_0)) \\
&\le G_{n-1}(|1-\gamma^*|+\tau_0+\frac{4}{v}\xi_{n-1}),
\end{aligned}$$

where we have used the fact that $|\xi_m^*-\xi_{m-1}^*|=\lambda|1-z|(\xi_m-\xi_{m-1})$ by (67), and, in the last inequality, (67), (83), and $|1-z|\le 2$.

Now, we divide both sides of (110) by $|1+\tau_0+\xi_o^*|$ and estimate

$$(111)|g_n| \le G_{n-1}\left\{\frac{|1-\gamma^*|+\tau_0}{|1+\tau_0+\xi_o^*|}+\frac{4\xi_{n-1}}{v|1+\tau_0+\xi_o^*|}\right\} \le G_{n-1}(1+\frac{4}{v}k\Xi(t_n)),$$

where we used Lemma 5.2(ii) and the monotonicity of ξ_n, (67).

The estimates above therefore suggest that the amplification sequence increases proportionally from one step to another by a factor of $1+O(k)$. This estimate is sharp in a sense that it can be seen by calculating exactly the amplification term g_2; unlike g_1 for which we have $|g_1|\le 1$, $|g_2|$ can be shown to exceed 1.

Remark 5. *When $D>0$, a straightforward modification in the calculations above can show that the inequalities* (103) *and* (111) *still hold with a denominator $|1+\tau_0+\xi_o^*+D_h|$, where $D_h=2D(1-\cos\theta)\frac{\lambda}{h}\ge 0$. Therefore, we can still prove the same bound for $|g_n|$, $n\ge 1$.*

Proposition 5.2. *Assume that the CFL condition,* (83)*, and the monotonicity of τ_m and ξ_m,* (66) *and* (67)*, respectively, hold. Then, the scheme* (100) *for* (99) *is weakly stable on $[0,t_n]$ for $t_n\le T$ and some T.*

Proof. The estimates preceding the statement of this proposition demonstrate that

$$|g_n| \le G_{n-1}(1+Ck),$$

where C depends only on Ξ and v. Via Bernoulli inequality, we have therefore

$$|g_n| \le (1+Ck)^{n-1} \le \exp(Ck(n-1)) \le \exp(CT),$$

that is, the amplification sequence is uniformly bounded. □

Remark 6. *From the proof of Proposition 5.2, it seems that, under additional assumptions on the relation of Ξ and v, one may be able to obtain strong stability. In particular, in the problem considered in this paper, we are likely to have $\xi_0=0$, and Ξ is likely to be bounded by some constant related to v. Under these assumptions, one may be able to group the terms ξ_m^* somehow along with v and avoid being left with ξ_{n-1}^* which causes the failure of strong stability. However, due to the complexity of the calculations in Section 4.3, we are unable to pursue this direction further at this time.*

5.7. Weak stability for $\Upsilon \not\equiv 0, \Psi \not\equiv 0, \Xi \not\equiv 0$. First, we set $\Xi \equiv 0$ and consider an extension of (78) for

$$u_t + \Upsilon * u_t - \Psi * u_{txx} + v u_x - D u_{xx} = 0. \tag{112}$$

We will include all the terms at the end.

Let us consider the new term $\Psi * u_{txx}$ first. The term $\Psi * u_{txx}$ is approximated in analogy to (65):

$$\begin{aligned}\Psi * u_{txx}|_{t=t_n, x=x_j} \approx \sum_{m=1}^{n} -\frac{1}{h^2}(2(u_{j,m} - u_{j,m-1}) - (u_{j-1,m} - u_{j-1,m-1}) \\ - (u_{j+1,m} - u_{j+1,m-1}))\psi_{n-m}\end{aligned}$$

With the above approximation, the scheme for (112) is

$$\begin{aligned}&(u_{j,n} - u_{j,n-1}) + \sum_{m=1}^{n}(u_{j,m} - u_{j,m-1})\tau_{n-m} \\ &+ \sum_{m=1}^{n} \frac{k}{h^2}\left(2(u_{j,m} - u_{j,m-1}) - (u_{j-1,m} - u_{j-1,m-1}) - (u_{j+1,m} - u_{j+1,m-1})\right)\psi_{n-m} \\ &\qquad + \lambda v(u_{j,n-1} - u_{j-1,n-1}) + D\frac{\lambda}{h}(2u_{j,n} - u_{j-1,n} - u_{j+1,n}) = 0.\end{aligned} \tag{113}$$

The stability analysis follows analogously to those in Propositions 5.1 and 5.2.

Proposition 5.3. *Let the CFL condition* (83) *hold and, further,* (66), (68a)–(68c) *be satisfied. Then, the scheme* (113) *is* ultra-weakly *stable that is,*

$$|g(k, \chi)| \leq 1 + g_\Psi(k), \, \forall \chi, \tag{114}$$

if (i) $g_\Psi(k) = \frac{k}{\psi_0} \to 0$ *as* $k \to 0$. *Alternatively, the scheme is weakly stable if (ii)* $\frac{k}{h^2} \leq \alpha$ *holds.*

Remark 7. *The result of Proposition 5.3 is weaker than that of the previous statements because of non-monotonicity of the kernels involved. In practice, however, we do not see a significant problem. If we let* $\Psi(t)$ *behave like* $t^{-1/2}$ *close to the origin, then* $\frac{k}{\psi_0} = g_\Psi(k) = O(\sqrt{k})$, *and the assumption (i) holds. Thus (ii) is not needed in practice.*

Proof. We can quickly derive difference equations for the amplification factors g_n using the same von-Neumann framework as in what led to (86). First, we define, for convenience,

$$\psi_m^* := \psi_m \frac{k}{h^2}(2 - z - \bar{z}) = \psi_m \frac{\lambda}{h} 2(1 - cos\theta), \; m = 0, 1, \ldots. \tag{115}$$

We note that all $\psi_m^* \in \mathbb{R}$ and are in fact nonnegative by Remark 3. Also, for a fixed θ, they are decreasing as long as $m \leq m_*$ and increasing for $m > m^*$.

For our analysis, we first set $D = 0$. Using (113) for $n = 1$, we obtain for g_1 that

$$(1 + \tau_0 + \psi_0^*)(v_1 - v_0) + v_0 \gamma^* = 0. \tag{116}$$

In order to estimate $|g_1|$, we proceed similarly as in (88), except that we replace τ_0 by $\tau_0 + \psi_0^*$. Then, as long as (83) holds, we have that, for any θ, $|g_1| \leq 1$. Next, for $n > 1$, we take similar steps to the ones leading to (94) in the proof of

Proposition 5.1, except that τ_m is replaced in each instance by $\tau_m + \psi_m^*$:

$$(1+\tau_0+\psi_0^*)|g_n| \le |1+\tau_0+\psi_0^*-\tau_1-\psi_1^*-\gamma^*||g_{n-1}| + \sum_{m=1}^{n-2}|g_m|(|\tau_{n-m}-\tau_{n-m-1}|+|\psi_{n-m}^*-\psi_{n-m-1}^*|)+|g_0|(\tau_{n-1}+\psi_{n-1}^*). \tag{117}$$

If $n < m_*$, we proceed in the same manner as in the remainder of the proof of Proposition 5.1 since we can telescope and cancel $\tau_m + \psi_m^*$ by the monotonicity of ψ_m. Therefore, for $n < m_*$, we can then easily obtain strong stability, i.e., $|g_n| \le 1$.

However, if $n > m_*$, the estimates differ from those following (94) or (109) since ψ_m^* is not monotone, and therefore the sign of $\psi_{n-m}^* - \psi_{n-m-1}^*$ changes at $m = m_*$, making the telescoping and cancellation of all the terms impossible. Nevertheless, we can still get weak stability by writing out the terms carefully.

We define $G_{n-1} := \max_{m=0,\dots n-1}|g_m|$ and recall the basic steps that were used to get (110) to see

$$\begin{aligned}(1+\tau_0+\psi_o^*)|g_n| \le G_{n-1}\{&|1-\gamma^*| \\ &+(\tau_0-\tau_1)-(\tau_{n-1}-\tau_{n-2})-(\tau_{n-2}-\tau_{n-3})-\dots-(\tau_2-\tau_1)+\tau_{n-1} \\ &+|\psi_0^*-\psi_1^*|+|\psi_{n-1}^*-\psi_{n-2}^*|+|\psi_{n-2}^*-\psi_{n-3}^*|+\dots+|\psi_2^*-\psi_1^*|+|\psi_{n-1}^*|\}.\end{aligned} \tag{118}$$

Note that, by (68a)–(68c), we have $\psi_{m_*}^* - \psi_{m_*-1}^* \le 0$, but $\psi_{m_*+1}^* - \psi_{m_*}^* \ge 0$.

Therefore, the summation of the absolute values on the right hand side of (118), after rearranging the terms, can be rewritten as

$$\begin{aligned}&|\psi_0^*-\psi_1^*|+|\psi_1^*-\psi_2^*|+\dots+|\psi_{m_*-1}^*-\psi_{m_*}^*|+|\psi_{m_*}^*-\psi_{m_*+1}^*| \\ &+\dots+|\psi_{n-3}^*-\psi_{n-2}^*|+|\psi_{n-2}^*-\psi_{n-1}^*|+|\psi_{n-1}^*| \\ =&\psi_0^*-\psi_1^*+\psi_1^*-\psi_2^*+\dots+\psi_{m_*-1}^*-\psi_{m_*}^*+\psi_{m_*+1}^*-\psi_{m_*}^*+\dots \\ &+\psi_{n-2}^*-\psi_{n-3}^*+\psi_{n-1}^*-\psi_{n-2}^*+\psi_{n-1}^* \\ =&2\psi_{n-1}^*-2\psi_{m_*}^*+\psi_0^*.\end{aligned} \tag{119}$$

Then, we obtain from (118) that

$$(1+\tau_0+\psi_o^*)|g_n| \le G_{n-1}\left\{|1-\gamma^*|+\tau_0+\psi_0^*+2(\psi_n^*-\psi_{m_*}^*)\right\}.$$

We will prove a similar bound as in (111), with a bit more work and extra assumptions need for the last term $(\psi_n^* - \psi_{m_*}^*)$ in the above inequality, which we discuss below.

There are two avenues to deal with this term. The first i) assumes (reasonable) bound on the growth of Ψ at the origin and leads to "ultra-weak" stability (114). The second ii) restricts the time step k and gives the usual weak stability (75).

To pursue i), we notice by (115) that the ratio $\frac{\psi_n^*-\psi_{m_*}^*}{1+\tau_0+\psi_0^*}$ can be bounded by $\frac{\psi_n^*-\psi_{m_*}^*}{\psi_0^*} = \frac{\psi_n-\psi_{m_*}}{\psi_0}$. Now, we take advantage of (56) and see that for $n > m*$ it is reasonable to estimate, since Ψ' is at least bounded by some D_* for $t > t_*$,

$$0 \le \psi_n - \psi_{m_*} = k(\Psi_n - \Psi_{m_*}) = k(k(n-m^*))\frac{\Psi_n - \Psi_{m_*}}{k(n-m^*)} \le kTD_*.$$

Next, we estimate the ratio

$$\frac{\psi_n - \psi_{m_*}}{\psi_0} \le \frac{k}{\psi_0}TD_*.$$

Thus, as long as $g_\Psi(k) = \frac{k}{\psi_0} \to 0$ as $k \to 0$, we have the *ultra-weak stability* (114).

The second approach ii) is simply to assume $\frac{k}{h^2} \leq \alpha$ for some constant α. This is similar to time step restrictions imposed for explicit diffusion schemes. While this choice of time step can be prohibitively expensive, stability analysis is very simple by noticing

$$\frac{\psi_n^* - \psi_{m_*}^*}{1 + \tau_0 + \psi_0^*} \leq \psi_n^* - \psi_{m_*}^* \leq 4\alpha k \max_{t \geq t_*} \Psi(t) = O(k),$$

and thus the weak stability is established.

The proof of Proposition 5.3 can be completed after we redo the calculation including $D \neq 0$. □

Now, combining the results and elements of the proof of Propositions 5.1, 5.2, and 5.3, we obtain the following theorem.

Theorem 5.1. *The following upwind-memory scheme for* (51)

$$\begin{aligned}
&(u_{j,n} - u_{j,n-1}) + \sum_{m=1}^{n} (u_{j,m} - u_{j,m-1})\tau_{n-m} \\
&+ \sum_{m=1}^{n} \frac{k}{h} \left((u_{j,m} - u_{j,m-1}) - (u_{j-1,m} - u_{j-1,m-1}) \right) \xi_{n-m} \\
&+ \sum_{m=1}^{n} \frac{k}{h^2} (2(u_{j,m} - u_{j,m-1}) \\
&- (u_{j-1,m} - u_{j-1,m-1}) - (u_{j+1,m} - u_{j+1,m-1}))\psi_{n-m} \\
&+ \lambda v (u_{j,n-1} - u_{j-1,n-1}) + D\frac{\lambda}{h}(2u_{j,n} - u_{j-1,n} - u_{j+1,n}) = 0. \qquad (120)
\end{aligned}$$

is weakly stable (or ultra-weakly stable) under the assumptions of Propositions 5.1, 5.2, and 5.3.

5.8. Stability analysis using MOL. We recall that von-Neumann analysis applies to homogeneous pure Cauchy problems on unbounded domains or to initial boundary value problems problems with periodic boundary conditions. The problem (51) we study in this paper is defined in practice on bounded domains with practical (other than periodic) boundary conditions. Thus in this section we consider the MOL approach as an alternative to von-Neumann stability analysis; it allows to understand stability and error propagation for inhomogeneous problems; this also helps to understand how the errors, e.g., truncation errors, may propagate in time. While we do not address the case of general boundary conditions, we set the framework for future extensions.

A general case of MOL applied to (51) is with (69) in which $u_n \in V$, and (69) is an equation (or a system) on an infinite dimensional Hilbert space V, and where V is selected appropriately for the given boundary value problem, and $C(k)$ is an abstract linear operator on V. This setup was used for self-adjoint problems, e.g., in [18] and allows to study semi-discrete error estimates and stability. Since our problem (51) is not self-adjoint due to the presence of $v \neq 0, \Xi \neq 0$, the techniques and set-up of [18] do not apply.

We pursue MOL analysis therefore only for a fully discrete version, i.e., for (69) is where $u_{j,n} \in \mathbb{R}$, $j = 1, \ldots J$, $u_n = (u_{1,n}, u_{2,n}, \ldots, u_{J,n})^T \in \mathbb{R}^J, C(k) \in \mathbb{R}^{J \times J}$. Still, some of the calculations below are similar to those in [18] even though the latter uses a rectangular rule and requires boundedness of the kernels, and requires

that the spatial operators involved are self-adjoint. On the other hand, [18] allow for the study in a general Hilbert space V while we only deal with the case $V = \mathbb{R}^J$.

Our MOL analysis is only performed for the (simple) case of periodic boundary conditions. For a non-self-adjoint problem, realistic boundary conditions imposed in (51) of Dirichlet and/or Neumann type render $C(k)$ to be nonnormal (see, e.g., [8]) and make any spectral analysis of $C(k)$ very complicated. Since the focus of this paper is on the influence of memory terms rather than on handling boundary conditions, we assume for simplicity only periodic boundary conditions. This makes the analysis of $C(k)$ similar to that of amplification factors g in von-Neumann analysis, and allows us to skip many details. Our MOL setup can be perhaps extended in future to handle nonperiodic boundary conditions.

For now, we assume that $\Xi \equiv 0$ and $\Psi \equiv 0$. We first rewrite (97) in matrix-vector form, to be satisfied by vector u_n as follows:

$$(121)\quad (u_n - u_{n-1}) + \lambda v \mathcal{A} u_{n-1} + \frac{Dk}{h^2}\mathcal{A}_d u_n + \sum_{m=1}^{n} (u_m - u_{m-1})\tau_{n-m} = 0,$$

where

$$(122)\qquad \mathcal{A} := \begin{bmatrix} 1 & & & & & -1 \\ -1 & 1 & & & & \\ & -1 & 1 & & & \\ & & \ddots & \ddots & & \\ & & & -1 & 1 & \\ & & & & -1 & 1 \end{bmatrix}$$

is the upwind difference operator matrix. It is well known [[8], *10.2, 10.4*] that $\mathcal{A}$ can be written as a sum of a scaled (circulant) matrix appropriate for centered difference and a scaled (symmetric nonnegative definite) diffusion matrix

$$(123)\qquad \mathcal{A}_d := \begin{bmatrix} 2 & -1 & & & & -1 \\ -1 & 2 & -1 & & & \\ & -1 & 2 & -1 & & \\ & & \ddots & \ddots & \ddots & \\ & & & -1 & 2 & -1 \\ -1 & & & & -1 & 2 \end{bmatrix}.$$

Also, it is known that $\mathcal{A}$ and $\mathcal{A}_d$ have the same orthogonal sets of eigenvectors, thus, in particular, that both are normal. We also recall that the eigenvalues of $\mathcal{A}$ and $\mathcal{A}_d$ are, respectively, $1 - z = 1 - e^{-i\theta}$ (see (85)) and $2(1 - \cos(\theta))$, where $0 \le \theta \le 2\pi$ runs through a discrete set of equidistant J angles.

5.8.1. Assume first that $D = 0$. For MOL stability analysis, we consider the inhomogeneous version of (121) and include kf_n on its right hand side to account for the anticipated collection of truncation errors that may arise as in (70) modifying (69). After rearranging terms, we get a vector equation of structure analogous to (93):

$$\begin{aligned}(1+\tau_0)u_n =& (1+\tau_0)u_{n-1} - \lambda v \mathcal{A} u_{n-1} - \tau_1 u_{n-1} \\ & - \sum_{m=1}^{n-2} u_m(\tau_{n-m} - \tau_{n-m-1}) + u_0\tau_{n-1} + kf_n.\end{aligned}$$

Set

$$\mathcal{C} := \frac{1}{1+\tau_0}((1+\tau_0)\mathbf{I} - \lambda v\mathcal{A})) = \mathbf{I} - \frac{\lambda v}{1+\tau_0}\mathcal{A}$$

and

$$(124) k\bar{f}_n := \frac{1}{1+\tau_0}(kf_n - \tau_1 u_{n-1} - \sum_{m=1}^{n-2} u_m(\tau_{n-m} - \tau_{n-m-1}) + u_0\tau_{n-1}).$$

Then, we get

$$u_n = \mathcal{C}u_{n-1} + k\bar{f}_n. \tag{125}$$

Iterating on (125), we obtain

$$u_n = C^n u_0 + k\sum_{m=0}^{n-1} C^{n-m+1}\bar{f}_m. \tag{126}$$

Since $\mathcal{A}$ is normal, $\mathcal{C}$ is normal as well. Thus, the analysis of stability, i.e., of bounds on $\mathcal{C}^n$ is equivalent to finding the bounds the eigenvalues of $\mathcal{C}$. In practice, similar book-keeping is needed as that we used to prove bounds on amplification factors G^n pursued in Section 5.4.

If k is chosen to satisfy the CFL condition, for each eigenvalue $\lambda(C) = 1 - \frac{v\lambda}{1+\tau_0}(1-z)$ of C with $z = e^{-i\theta}$, we have by Lemma 5.1 that $|\lambda(C)| \leq 1$ and hence $\|C^n\| \leq 1$. Therefore, we obtain

$$\|u_n\| \leq \|u_0\| + k\sum_{j=0}^{n-1}\|\bar{f}_j\|. \tag{127}$$

Note that $\|\bar{f}_j\|$, $j = 0, \ldots, n-1$, include the telescoping entries involving u_m, so that (127) does not complete the stability proof. However, one could proceed by induction similarly as was done in the proof of Proposition 5.1 to obtain strong stability for the homogeneous case, i.e., $\|u_n\| \leq \|u_0\|$. We skip the details because they do not bring any new information.

For the inhomogeneous case, we proceed similarly as in [18] and obtain weak stability via a calculation that can be later applied immediately to the cases with $\Xi \neq 0, \Psi \neq 0$.

To this aim, we prove the following auxiliary Lemma.

Lemma 5.3. *Let u_n satisfy* (127) *and*

$$k\|\bar{f}_n\| \leq k\|f_n\| + \sum_{m=0}^{n-1}\alpha_{n-1-m}\|u_m\| \tag{128}$$

for some given nonnegative sequence $(\alpha_m)_{m=0}^{n-1}$ whose sum for any n is bounded by some constant α^*. Then, there is a constant C_T which depends only on kt_n and on $(\alpha_m)_m$ such that

$$\|u_n\| \leq C_T(\|u_0\| + \sum_{m=0}^{n}\|f_m\|).$$

Proof. By (127), we get

$$\|u_n\| \leq \|u_0\| + k\sum_{j=0}^{n-1}\|f_j\| + k\sum_{j=0}^{n-1}\sum_{m=0}^{j-1}\alpha_{j-1-m}\|u_m\|. \tag{129}$$

We switch the order of summation in the last sum of (129) to obtain

$$\sum_{j=0}^{n-1}\sum_{m=0}^{j-1}\alpha_{j-1-m}\|u_m\| = \sum_{m=0}^{n-1}\|u_m\|\sum_{j=m+1}^{n}\alpha_{j-1-m}.$$

Then, since α_{jk} are all nonnegative and their sum is bounded, we can estimate from (129)

$$\|u_n\| \le \|u_0\| + k\sum_{j=0}^{n-1}\|f_j\| + k\alpha^*\sum_{m=0}^{n-1}\|u_m\|. \tag{130}$$

Applying discrete Gronwall's Lemma as in [[18], *Lemma preceding Theorem 1*], we conclude that

$$\|u_n\| \le C_T\left(k\sum_{m=0}^{n-1}\|f_m\| + \|u_0\|\right), \tag{131}$$

where the constant C_T depends only on $T = nk$ and α^*. □

Now, we can use Lemma 5.3 with

$$\alpha_{n-1-m} = |\tau_{n-m} - \tau_{n-m-1}|,\ m = 1,\dots n-2,\ \alpha_{n-1} = \tau_{n-1},\ \alpha_1 = \tau_1. \tag{132}$$

We see that these coefficients are nonnegative and that their sum is bounded by $\sum_{m=0}^{n}\tau_m = \int_0^{t_n}\Upsilon(s)ds$ which by Remark 1 is bounded. Thus, we obtain (131), i.e., weak stability.

5.8.2. The analysis above is easily extended to the case $D \neq 0$. In this case, by setting

$$\begin{aligned}\mathcal{B} &:= (1+\tau_0)\mathbf{I} + \frac{Dk}{h^2}\mathcal{A}_d,\\ \mathcal{G} &:= I(1+\tau_0) - \lambda v\mathcal{A}),\\ \mathcal{C} &:= \mathcal{B}^{-1}\mathcal{G},\end{aligned}$$

we can see that (125) still holds and we have to prove that $\|\mathcal{C}\| \le 1$ like in the previous case. We notice that $\mathcal{B}$ and $\mathcal{G}$ have the same (full) set of eigenvectors, thus the eigenvalues of $\mathcal{C}$ are the ratio of those for $\mathcal{G}$ and $\mathcal{B}$. In order to find conditions upon which $\|\mathcal{C}\| \le 1$, we analyze the magnitude of the eigenvalues

$$\frac{|1+\tau_0 - \lambda v(1-z)|}{|1+\tau_0 + \frac{Dk}{h^2}2(1-\cos(\phi))|}.$$

Since the denominator is real and bounded from below by $1+\tau_0$, Lemma 5.1 implies that the CFL condition (83) is sufficient for the above expression to be bounded by 1, and hence for stability.

The arguments used to demonstrate $\|\mathcal{C}\| \le 1$ are similar to those in von-Neumann Ansatz.

5.8.3. The MOL analysis for the cases $\Upsilon \neq 0, \Xi \neq 0, \Psi \neq 0$, which gives weak stability as long as (83) holds, is somewhat more involved, but eventually follows from Lemma 5.3.

We formulate the scheme (113) in the MOL framework as follows:

$$(u_n - u_{n-1}) + \lambda v \mathcal{A} u_{n-1} + \frac{Dk}{h^2}\mathcal{A}_d u_n$$
$$+\sum_{m=1}^{n} \tau_{n-m}(u_m - u_{m-1}) + \sum_{m=1}^{n} \lambda\xi_{n-m}\mathcal{A}(u_m - u_{m-1}) + \sum_{m=1}^{n} \frac{k}{h^2}\psi_{n-m}\mathcal{A}_d(u_m - u_{m-1}) = 0.$$

We can rewrite the above equation to see

$$\left((1+\tau_0)\mathbf{I} + \frac{k}{h^2}(D+\psi_0)\mathcal{A}_d + \lambda\xi_0\mathcal{A}\right) u_n = \left((1+\tau_0)\mathbf{I} + \frac{k}{h^2}\psi_0\mathcal{A}_d - \lambda(v-\xi_0)\mathcal{A}\right) u_{n-1} + k\tilde{f}_n \tag{133}$$

with

$$k\tilde{f}_n := kf_n - (\tau_1\mathbf{I} + \frac{k}{h^2}\psi_1\mathcal{A}_d + \lambda\xi_1\mathcal{A})u_{n-1}$$
$$-\sum_{m=1}^{n-2}\left((\tau_{n-m} - \tau_{n-m-1})\mathbf{I} + \frac{k}{h^2}(\psi_{n-m} - \psi_{n-m-1})\mathcal{A}_d + \lambda(\xi_{n-m} - \xi_{n-m-1})\mathcal{A}\right) u_m$$
$$+ (\tau_{n-1}\mathbf{I} + \frac{k}{h^2}\psi_{n-1}\mathcal{A}_d + \lambda\xi_{n-1}\mathcal{A})u_0.$$

To put this in the form (125), we set

$$\begin{aligned}
\mathcal{B} &:= (1+\tau_0)\mathbf{I} + \frac{k}{h^2}(D+\psi_0)\mathcal{A}_d + \lambda\xi_0\mathcal{A} \\
\mathcal{G} &:= (1+\tau_0)\mathbf{I} + \frac{k}{h^2}\psi_0\mathcal{A}_d - \lambda(v-\xi_0)\mathcal{A} \\
\mathcal{C} &:= \mathcal{B}^{-1}\mathcal{G}.
\end{aligned}$$

and

$$\bar{f_n} := \mathcal{B}^{-1} f_n.$$

If we assume $\xi_0 = 0$, it is easy to prove that $\|\mathcal{C}\| \leq 1$ l in a manner similar to what was done in Section 5.8.2. However, we need also to consider the norms of $\mathcal{B}^{-1}\mathcal{G}_m$, where $\mathcal{G}_m$ are the matrices appearing in the definition of $\tilde{f_n}$ such that

$$k\tilde{f}_n := kf_n - \mathcal{G}_{n-1}u_{n-1} - \sum_{m=1}^{n-2}\mathcal{G}_m u_m + \mathcal{G}_0 u_0.$$

However, these norms are not bounded by 1 but rather by $1 + C_\Xi k$, where C_Ξ is a constant depending on Ξ. This can be seen in a similar way to the estimate (111).We proceed next to estimate the terms $\|\bar{f_n}\|$ in a similar manner to Lemma 5.3, with α_m including appropriate components involving $C_\Xi, \tau_p, \xi_p, \psi_p$ for appropriate p, in analogy with (132). Analysis for $\xi_0 \neq 0$ will not be presented.

We summarize the results in the following theorem, which extends Theorem 5.1 to the nonhomogeneous case.

Theorem 5.2. *Supposed that the same assumptions of Theorem 5.1 and an additional assumption* (54) *are satisfied. Then, the solutions to the upwind memory scheme* (120)*, when extended to the inhomogeneous case, satisfy the weak stability bound*

$$\|u_n\| \leq C\left(k\sum_{m=0}^{n}\|f_m\| + \|u_0\|\right), \tag{134}$$

TABLE 1. Simulation parameters.

Domain $[cm^2 \times min]$	$\Omega = [0, 40] \times [0, 10]$	[0, T]=[0, 1800]
Generic cell $[cm^2]$	$l = 2.5, 5.0$	$\delta = 0.2$
Porosity [-]	$\phi_f = 0.42$	$\phi_s = 0.42$
Permeability $[cm/min]$	$\mathbf{K}_f = 9.647$	$\mathbf{K}_s = \mathbf{K}_f/\mathbf{K}_{ratio}$
Diffusivity $[cm^2/min]$	$d_{\mathrm{m}} = 3.4 \cdot 10^{-4}$	
Dispersivity $[cm]$	$d_{\mathrm{t}} = 0.15$	$d_{\mathrm{l}} = 1.5$

where C is some constant only depending on Υ, Ξ, Ψ, and the final time T.

6. Numerical Results

In this section, we present some numerical results to validate our upscaled solute transport model (17) in 2d space. For simulations of the micro-model, we used the first-order Godunov and cell-centered finite difference (CCFD) method combined with backward Euler discretization in time, see [3, 4]. These techniques are well known to be first order accurate in time and space. Our implementation in MATLAB is similar to that described in [2, 16]. On the other hand, we implemented CCFD and a Locally Conservative Eulerian-Lagrangian Method (LCELM)[6, 5, 7] to discretize the systems (10) and (12), and the effective solute transport equation (17).

It is well known that advection-dominated PDEs present serious numerical difficulties due to the moving steep fronts present in the solutions of advection-diffusion transport PDEs or shock discontinuities in the solutions of pure hyperbolic PDEs. In response to this, a variety of numerical techniques have been introduced, with many classified as Eulerian-Lagrangian methods, in which an Eulerian finite difference or finite element treatment of diffusion is combined with a Lagrangian treatment of convection. LCELM is one that was especially designed to achieve local mass conservation. However, with the extra memory terms in our upscaled model, we observed from our simulation results that LCELM and CCFD yield almost identical results. Therefore, we neither describe the algorithms of LCELM nor present the results from LCELM here.

Assume that $\widetilde{\Omega} = (0, L_x) \times (0, L_y)$. We introduce the grid for the CCFD for which we partition $\widetilde{\Omega}$ into a uniform rectangular cells as follows: Let $N_x > 0$ and $N_y > 0$ be integers and $\Delta x = L_x/N_x$ and $\Delta y = L_y/N_y$. Let $x_i = i\Delta x$ and $y_j = j\Delta y$, $i = 0, \cdots, N_x$, $j = 0, \cdots, N_y$ and define the cells to be the rectangles $K_{ij} = (x_{i-1}, x_i) \times (y_{j-1}, y_j)$, $i = 1, \cdots, N_x$, $j = 1, \cdots, N_y$ with the centers $z_{i,j} = (x_{i-1} + 0.5\Delta x, y_{j-1} + 0.5\Delta y)$. For the temporal discretization, we use k to denote the time step, so $t^n = nk$, $n = 1, \cdots, N_t$.

We want to compute an approximate solution $u^n_{i,j} \approx u(z_{i,j}, t^n)$, $i = 0, \cdots, N_x$, $j = 0, \cdots, N_y$ at each discrete time step t^n, $n = 1, \cdots, N_t$.

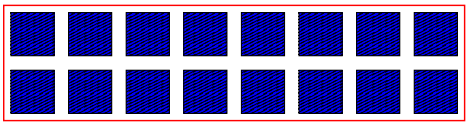

FIGURE 2. Computational domain Ω with 8 by 2 matrix blocks.

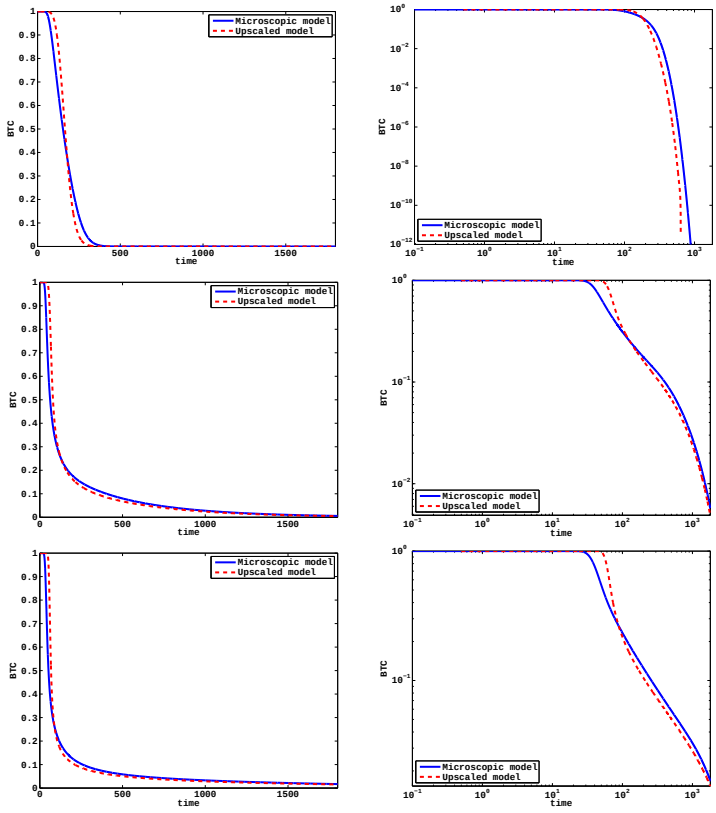

FIGURE 3. Breakthrough curves from the microscopic and upscaled models on linear (left column) and log-log scale (right column) when the domain has 8 by 2 matrix blocks. The low, intermediate, and high contrast cases ($\mathbf{K}_{ratio} = 6, 300, 1800$, respectively) from top to bottom.

For the spatial discretization, the diffusion terms, both primary and secondary, are approximated using the standard 5 point finite difference formula:

$$\nabla \cdot (\mathbf{D}\nabla u) \mid_{(z_{i,j},t^n)} \approx \frac{1}{\Delta x}\left(D_{i+1/2,j}\frac{u^n_{i+1,j}-u^n_{i,j}}{\Delta x} - D_{i-1/2,j}\frac{u^n_{i,j}-u^n_{i-1,j}}{\Delta x}\right) + \frac{1}{\Delta y}\left(D_{i,j+1/2}\frac{u^n_{i,j+1}-u^n_{i,j}}{\Delta y} - D_{i,j-1/2}\frac{u^n_{i,j}-u^n_{i,j-1}}{\Delta y}\right),$$

where the diffusion coefficients, $D_{i\pm1/2,j}$ and $D_{i,j\pm1/2}$, at the cell interfaces are given by the harmonic average of the adjacent cell-center diffusion coefficients. For example,

(135)
$$D_{i-1/2,j} = \left[\frac{1}{2}\left(\frac{1}{D_{i-1,j}} + \frac{1}{D_{i,j}}\right)\right]^{-1}, \quad D_{i,j-1/2} = \left[\frac{1}{2}\left(\frac{1}{D_{i,j-1}} + \frac{1}{D_{i,j}}\right)\right]^{-1}.$$

On the other hand, the advection terms are approximated using the upwind scheme and treated explicitly.

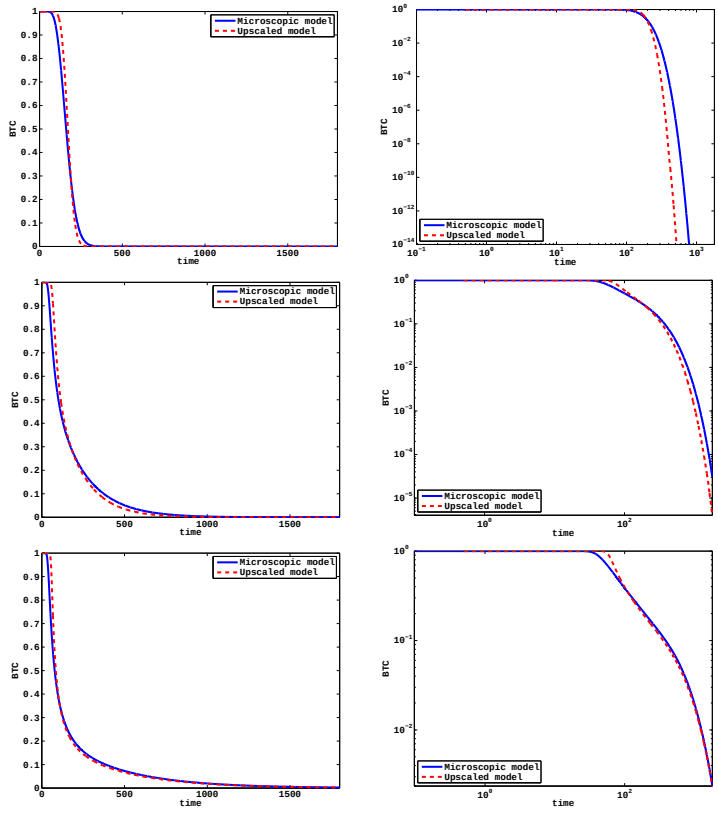

FIGURE 4. Breakthrough curves from the microscopic and upscaled models on linear (left column) and log-log scale (right column) when the domain has 16 by 4 matrix blocks. The low, intermediate, and high contrast cases ($\mathbf{K}_{ratio} = 6, 300, 1800$, respectively) are given from top to bottom.

Now, we will describe how to approximate the memory (convolution) terms. Each convolution term in the upscaled model (17) is of the form

$$(\mathcal{G} * \mathcal{L}u_t)(\mathbf{x}, t) = \int_0^t \mathcal{G}(t-s)\mathcal{L}u_t(\mathbf{x}, s)\, ds, \mathbf{x} \in \widetilde{\Omega}, t \in I = (0, T],$$

where $\mathcal{G} = \Upsilon, \Xi$, or Ψ and $\mathcal{L}$ is one of the identity, diffusion, or advection operators. We use an appropriately modified version of the product integration rule (61) for each convolution term:

$$(\mathcal{G} * \mathcal{L}u_t)(z_{i,j}, t^n) \approx \sum_{m=1}^{n} \frac{\mathcal{L}_h u_{i,j}^m - \mathcal{L}_h u_{i,j}^{m-1}}{m} g_{n-m}, \tag{136}$$

where $\mathcal{L}_h$ is a discrete operator corresponding to $\mathcal{L}$ and $g = \tau, \xi$, or ψ. More specifically, if $\mathcal{L}$ is a diffusion operator, $\mathcal{L}_h$ is the standard 5-point finite difference scheme and if $\mathcal{L}$ is an advection operator, $\mathcal{L}_h$ is the upwind finite difference scheme.

For our simulations, we used a rectangular domain Ω of size $40 \times 10\, cm^2$. Let the generic cell Ω_0 be a square of size $l \times l$, and Ω_{0s}, centered inside Ω_0, be a square of size $(l-\delta) \times (l-\delta)$. Therefore, the fast flow part Ω_{0f} has uniform thickness around

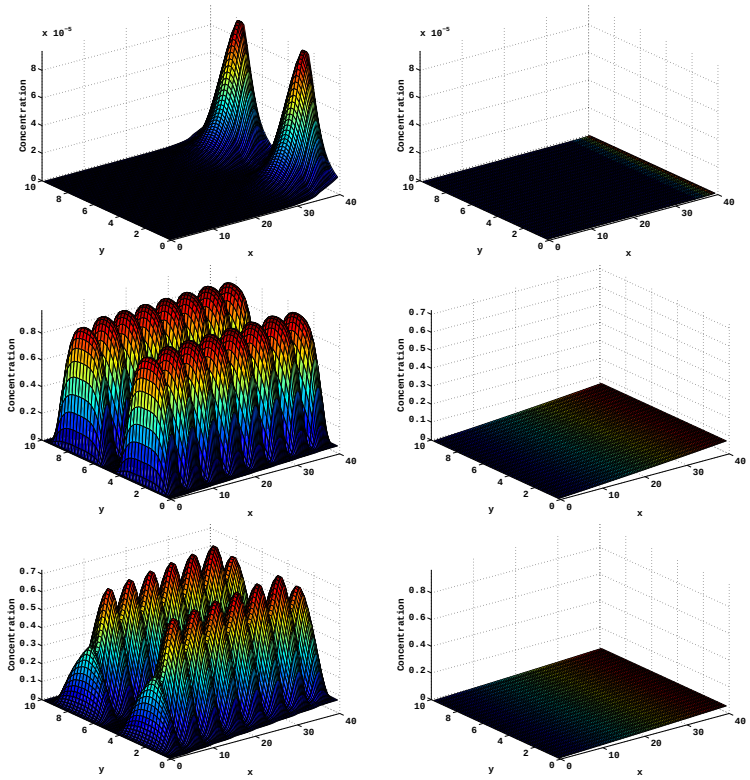

FIGURE 5. Concentration solutions at time $T = 500$ from the microscopic and upscaled models for $\mathbf{K}_{ratio} = 6, 300, 1800$ are given from top to bottom.

Ω_{0s}. An example computational domain with 8 by 2 matrix blocks is depicted in Fig 2.

The fast flow region, Ω_f, and the slow flow region, Ω_s, have the same porosity of $\phi_f = \phi_s = 0.42$. Here, we consider three different regimes of flow and transport depending on the ratio $\mathbf{K}_{ratio} = \mathbf{K}_f/\mathbf{K}_s$: $\mathbf{K}_{ratio} = 6, 300, 1800$. We assume that the permeability $\mathbf{K}_f$ is isotropic and $\mathbf{K}_f = 9.647\, cm/min$. We also assume that the medium is initially fully concentrated with the solute, i.e. $u^*(\mathbf{x}, 0) = 1$, $\mathbf{x} \in \Omega$ and clear fluid is pumped $\mathbf{v}_f \cdot \mathbf{n} = -v_l = -3.4 \cdot 10^{-4}\, [cm/min]$ along the left boundary and $\mathbf{v}_f \cdot \mathbf{n} = v_r = 3.4 \cdot 10^{-4}\, [cm/min]$ along the right boundary of the medium. Our simulation parameters are summarized in Table 1.

In our simulation, we approximate the effective permeability $\mathbf{K}^*$ with simple formula used by Arbogast [1], which is averaging the microscopic permeability harmonically in the direction of flow and arithmetically in the transverse direction. In our problem, the effective permeability can be approximated by $\mathbf{K}^* = \frac{\delta}{l} \cdot \mathbf{K}_f$. The effective diffusion/dispersion tensor is computed in the same way, *i.e.* $\mathbf{D}^* = \frac{\delta}{l} \cdot \mathbf{D}(\mathbf{v}^*)$.

Due to the boundary conditions for $\mathbf{v}_f$, our effective flow problem (9) becomes an 1-D problem which yields $\overline{\mathbf{v}^*} = (v_l, 0) = (3.4 \cdot 10^{-4}, 0)$. Then, $\mathbf{v}^* = (v_l \mathbf{K}^*/(\mathbf{K}^* + \theta_s \mathbf{K}_s), 0)$ and $\mathbf{v}_i^* = (v_l \mathbf{K}_s/(\mathbf{K}^* + \theta_s \mathbf{K}_s), 0)$ follow from (8) and (9).

First, in order to validate our upscaled model, we compare breakthrough curves produced by the microscopic model (1) and (2) and the ones produced by our

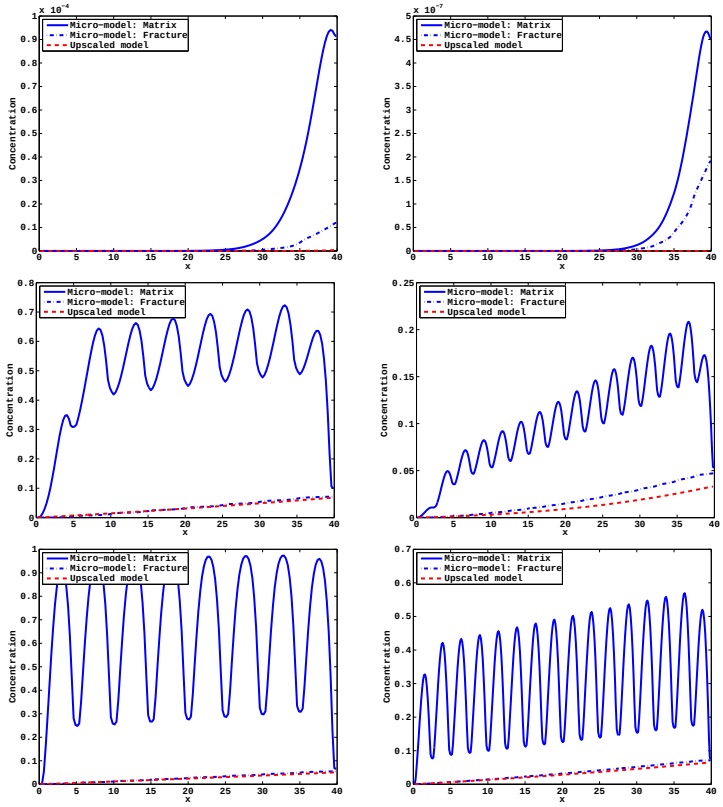

FIGURE 6. Cross-sections of the concentration profile from the microscopic and upscaled models when the domain has 8 by 2 matrix blocks (left column) and 16 by 4 matrix blocks (right column) for $\mathbf{K}_{ratio} = 6, 300, 1800$ from top to bottom.

upscaled model (9) and (17). The breakthrough curves are measured at the outlet (right side) of the medium with 8×2 blocks ($l = 5.0$) and 16×4 blocks ($l = 2.5$). The upscaled model was solved as described earlier in this section and the microscopic model was solved by the cell-centered finite difference (CCFD) method.

Figure 3 depicts the comparison of breakthrough curves between the microscopic and upscaled models for various flow regimes on both linear scale (left column) and log-log scale (right column) when the domain has 8 by 2 matrix blocks. We observe that the breakthrough curves of the microscopic simulations using CCFD (blue solid lines) show a good match with that of the upscaled model (red dashed lines) throughout the whole range of $\mathbf{K}_{ratio}$ values. Moreover, breakthrough curves from different permeability heterogeneity display different tailing behaviors. No significant tailing occurs in the low contrast case ($\mathbf{K}_{ratio} = 6$). In the high contrast case ($\mathbf{K}_{ratio} = 1800$), the tailing is long-term and diffusion driven, while the intermediate contrast case ($\mathbf{K}_{ratio} = 300$) shows a flatter early part of tails which are primarily advective.These phenomena coincide with the observation made in lab experiments [21].

We also did the same comparison study when the domain has 16 by 4 blocks and the results are shown in Figure 4. We observe a better match between the two models when there are more matrix blocks. On the other hand, the tails in the

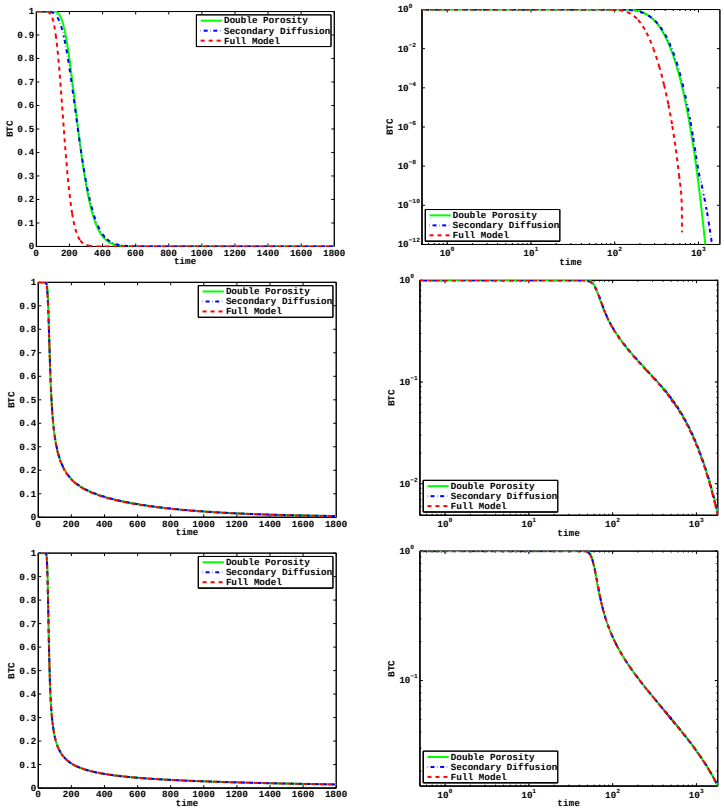

FIGURE 7. Breakthrough curves using various models from different permeability heterogeneity, $\mathbf{K}_{ratio} = 6, 300, 1800$ from top to bottom, on linear scale (left column) and log-log scale (right column).

intermediate and high contrast cases look qualitatively different from the previous case of 8 by 2 blocks.

Next, we compare the solution (concentration profile) of the microscopic model (left column) and the upscaled model (right column) at time $T = 500$ for the domain with 8 by 2 matrix blocks in Figure 5. The heterogeneous structure of Ω is apparent from the behavior of the microscopic model solution, which has a large concentration gradient on the matrix boundaries.

For a better comparison of the two models, Figure 6 illustrates cross-sections of the microscopic and upscaled models along the lines $y = 2.5$ (along the center of matrix blocks) and $y = 5$ (along the fracture) for the 8 by 2 matrix block case and along the lines $y = 1.25$ and $y = 2.5$ for the 16 by 4 matrix block case.

In order to examine the quantitative significance of each memory term in different regimes of flow and transport, we compare three different models; the traditional double porosity model, the model which includes the secondary diffusion term, $\nabla \cdot \left(\Psi * \nabla \frac{\partial u^*}{\partial t} \right)$, along with the double porosity term, $\mathcal{T}^{00} * \frac{\partial u^*}{\partial t}$, and the full model which includes all memory terms. In Figure 7, we depict the result for various permeability heterogeneity, $\mathbf{K}_{ratio} = 6, 300, 1800$. Across the whole range of $\mathbf{K}_{ratio}$ values, the secondary diffusion term is almost negligible. On the other hand, while

the secondary advection term, $\Xi * \nabla \frac{\partial c^*}{\partial t}$, is insignificant for the intermediate and high contrast cases ($\mathbf{K}_{ratio} = 300, 1800$), it plays an important role for the low contrast case ($K_{ratio} = 6$). Therefore, the traditional double-porosity model yields fairly good results for the intermediate and high contrast cases. However, in the low contrast cases, we need more memory terms to capture the dynamic in the breakthrough curves.

Acknowledgements

This work was supported by the grant DOE-98089 "Modeling, analysis, and simulation of preferential flow in porous media". Research of Peszyńska was also partially supported by the NSF-DMS-0511190 "Modeling adaptivity for porous media" and NSF-DMS 1115827 "Hybrid modeling in porous media."

References

[1] T. Arbogast, Gravitational forces in dual-porosity systems: Ii. computational validation of the homogenized model, Transport Porous Med., 13 (1993) 205–220.
[2] T. Arbogast, User Guide to Parssim1:The Parallel Subsurface Simulator, Single Phase, Version: Parssim1 v. 2.1, Technical report, Center for Subsurface Modeling, The University of Texas at Austin, 1998. (Minor updates to February 21, 2006).
[3] C. Dawson, Godunov-mixed methods for advective flow problems in one space dimension, SIAM J. Numer. Anal., 28 (1991) 1282–1309.
[4] C. Dawson, Godunov-mixed methods for advection-diffusion equations in multidimensions, SIAM J. Numer. Anal., 30 (1993) 1315–1332.
[5] J. Douglas, Jr. and C.-S¿ Huang, A locally conservative Eulerian-Lagrangian finite difference method for a parabolic equation, BIT, 41 (2001) 480–489.
[6] J. Douglas, Jr., F. Pereira, and L. M. Yeh, A locally conservative Eulerian-Lagrangian numerical method and its application to nonlinear transport in porous media, Comput. Geosci., 4 (2000) 1–40.
[7] J. Douglas, Jr., A. M. Spagnuolo, and S. Y. Yi, The convergence of a multidimensional, locally conservative Eulerian-Lagrangian finite element method for a semilinear parabolic equation, Math. Models Methods Appl. Sci., 20 (2010) 315–348.
[8] R. J. LeVeque, Finite difference methods for ordinary and partial differential equations, Society for Industrial and Applied Mathematics (SIAM), Philadelphia, PA, 2007. Steady-state and time-dependent problems.
[9] Y. P. Lin, V. Thomée, and L. B. Wahlbin, Ritz-Volterra projections to finite-element spaces and applications to integrodifferential and related equations, SIAM J. Numer. Anal., 28 (1991) 1047–1070.
[10] W. McLean and V. Thomée, Numerical solution of an evolution equation with a positive-type memory term, J. Austral. Math. Soc. Ser. B, 35 (1993) 23–70.
[11] W. McLean and V. Thomée, Asymptotic behaviour of numerical solutions of an evolution equation with memory, Asymptot. Anal., 14 (1997) 257–276.
[12] W. McLean, V. Thomée, and L. B. Wahlbin, Discretization with variable time steps of an evolution equation with a positive-type memory term, J. Comput. Appl. Math., 69 (1996) 49–69.
[13] M. Peszyńska, Finite element approximation of diffusion equations with convolution terms, Math. Comp., 65 (1996) 1019–1037.
[14] M. Peszynska, Numerical scheme for a conservation law with memory, Numerical Methods for PDEs, 30 (2014) 239–264.
[15] M. Peszyńska and R. E. Showalter, Multiscale elliptic-parabolic systems for flow and transport, Electron. J. Diff. Equations, 2007: No. 147, 30 pp. (electronic), 2007.
[16] M. Peszynska and S. Sun, Reactive transport module TRCHEM in IPARS, Technical report, TICAM Report 01-32, 2001.
[17] R. D. Richtmyer, Difference methods for initial-value problems. Interscience tracts in pure and applied mathematics. Iract 4, Interscience Publishers, Inc., New. York, 1957.
[18] I. H. Sloan and V. Thomée, Time discretization of an integro-differential equation of parabolic type, SIAM J. Numer. Anal., 23 (1986) 1052–1061.
[19] V. Thomée and L. B. Wahlbin, Long-time numerical solution of a parabolic equation with memory, Math. Comp., 62 (1994) 477–496.

[20] S. Y. Yi, M. Peszyńska, and R. Showalter, Numerical upscaled model of transport with non-separated scales. In Proceedings of CMWR XVIII in Barcelona, June 21-24, 2010, available online at http://congress.cimne.com/CMWR2010/Proceedings, 2010. paper 188.
[21] B. Zinn, L. C. Meigs, C. F. Harvey, R. Haggerty, Williams J. Peplinski, and Claudius Freiherr von Schwerin, Experimental visualization of solute transport and mass transfer processes in two-dimensional conductivity fields with connected regions of high conductivity, Environ Sci. Technol., 38 (2004) 3916–3926.

Department of Mathematics, Oregon State University, Corvallis, OR 97331, USA
E-mail: mpesz@math.oregonstate.edu

Department of Mathematics, Oregon State University, Corvallis, OR 97331, USA
E-mail: show@math.oregonstate.edu

Department of Mathematical Sciences, The University of Texas at El Paso, El Paso, TX 79968, USA
E-mail: syi@utep.edu